Stem Cell Reports
Article

ISSCR

OPEN ACCESS

Generation of Human Liver Chimeric Mice with Hepatocytes from Familial Hypercholesterolemia Induced Pluripotent Stem Cells

Jiayin Yang,[1,8,10] Yu Wang,[2,3,8,10] Ting Zhou,[2,3,8] Lai-Yung Wong,[1] Xiao-Yu Tian,[4] Xueyu Hong,[1] Wing-Hon Lai,[1] Ka-Wing Au,[1] Rui Wei,[1] Yuqing Liu,[2,3] Lai-Hung Cheng,[4] Guichan Liang,[2,3] Zhijian Huang,[2,3] Wenxia Fan,[2,3] Ping Zhao,[2,3] Xiwei Wang,[2,3] David P. Ibañez,[2,3] Zhiwei Luo,[2,3] Yingying Li,[2,3] Xiaofen Zhong,[2,3] Shuhan Chen,[2,3] Dongye Wang,[2,3] Li Li,[2] Liangxue Lai,[2] Baoming Qin,[2,5] Xichen Bao,[2,3] Andrew P. Hutchins,[6] Chung-Wah Siu,[1,7,8] Yu Huang,[4] Miguel A. Esteban,[2,3,8,*] and Hung-Fat Tse[1,7,8,9,*]

[1]The Cardiology Division, Department of Medicine, Li Ka Shing Faculty of Medicine, The University of Hong Kong, Hong Kong SAR, China
[2]CAS Key Laboratory of Regenerative Biology, Joint School of Life Sciences, Guangzhou Institutes of Biomedicine and Health, Chinese Academy of Sciences, Guangzhou 510530, and Guangzhou Medical University, Guangzhou 511436, China
[3]Laboratory of RNA, Chromatin, and Human Disease, CAS Key Laboratory of Regenerative Biology and Guangdong Provincial Key Laboratory of Stem Cells and Regenerative Medicine, Guangzhou Institutes of Biomedicine and Health, Chinese Academy of Sciences, Guangzhou 510530, China
[4]Institute of Vascular Medicine, Li Ka Shing Institute of Health Sciences, School of Biomedical Sciences, Chinese University of Hong Kong, Hong Kong SAR, China
[5]Laboratory of Metabolism and Cell Fate, CAS Key Laboratory of Regenerative Biology and Guangdong Provincial Key Laboratory of Stem Cells and Regenerative Medicine, Guangzhou Institutes of Biomedicine and Health, Chinese Academy of Sciences, Guangzhou 510530, China
[6]Department of Biology, Southern University of Science and Technology of China, Shenzhen 518055, China
[7]Research Centre of Heart, Brain, Hormone, and Healthy Ageing, Li Ka Shing Faculty of Medicine, The University of Hong Kong, Hong Kong SAR, China
[8]Hong Kong-Guangdong Stem Cell and Regenerative Medicine Research Centre, The University of Hong Kong and Guangzhou Institutes of Biomedicine and Health, Hong Kong SAR, China
[9]Department of Medicine, The University of Hong Kong-Shenzhen Hospital, Shenzhen 518053, China
[10]Co-first author
*Correspondence: miguel@gibh.ac.cn (M.A.E.), hftse@hku.hk (H.-F.T.)
http://dx.doi.org/10.1016/j.stemcr.2017.01.027

SUMMARY

Familial hypercholesterolemia (FH) causes elevation of low-density lipoprotein cholesterol (LDL-C) in blood and carries an increased risk of early-onset cardiovascular disease. A caveat for exploration of new therapies for FH is the lack of adequate experimental models. We have created a comprehensive FH stem cell model with differentiated hepatocytes (iHeps) from human induced pluripotent stem cells (iPSCs), including genetically engineered iPSCs, for testing therapies for FH. We used FH iHeps to assess the effect of simvastatin and proprotein convertase subtilisin/kexin type 9 (PCSK9) antibodies on LDL-C uptake and cholesterol lowering in vitro. In addition, we engrafted FH iHeps into the liver of *Ldlr*$^{-/-}$/*Rag2*$^{-/-}$/*Il2rg*$^{-/-}$ mice, and assessed the effect of these same medications on LDL-C clearance and endothelium-dependent vasodilation in vivo. Our iHep models recapitulate clinical observations of higher potency of PCSK9 antibodies compared with statins for reversing the consequences of FH, demonstrating the utility for preclinical testing of new therapies for FH patients.

INTRODUCTION

Mutations in *LDLR* (encoding LDL receptor, LDLR), often heterozygous, underlie most cases of familial hypercholesterolemia (FH), which predisposes to premature cardiovascular disease due to marked elevation of plasma levels of lipids, in particular low-density lipoprotein cholesterol (LDL-C) (Brown and Goldstein, 1986). Besides diet control and physical activity, FH patients are treated with statins, a class of drugs that inhibit 3-hydroxy-3-methylglutaryl-coenzyme A (HMG-CoA) reductase and hence reduce cholesterol synthesis in the liver (Endo, 1992). Statins also increase LDLR protein levels in hepatocytes and LDL-C clearance from plasma. Because of these properties, statins are used to treat FH patients and also patients with non-familial hypercholesterolemia. However, statins fail to reduce plasma LDL-C adequately in the majority of these patients for prevention of cardiovascular events (Cannon et al., 2015; Reiner, 2015), and a proportion of patients suffers from significant adverse effects (Dormuth et al., 2014; Stroes et al., 2015).

Importantly, FH can be caused by mutations in other genes besides *LDLR*, including gain-of-function mutations in proprotein convertase subtilisin/kexin type 9 (PCSK9) (Sniderman et al., 2014). This observation led to the subsequent identification of PCSK9 as an extracellular protein responsible for the internalization and degradation of surface LDLR in hepatocytes (Maxwell et al., 2005). Interestingly, PCSK9 is induced by statins, and activates a negative feedback loop that controls LDLR expression and consequently restrains the efficacy of statins (Dubuc et al., 2004). The latter may account for the limited efficacy or even loss of efficacy of statins in some patients, and has suggested that PCSK9 modulation could be of therapeutic relevance. In this regard, clinical trials with

anti-PCSK9 therapy (in the form of monoclonal antibodies) have shown potent lowering effects on LDL-C and good tolerance, creating a tremendous interest in this approach as an alternative medication for hypercholesterolemia (Robinson et al., 2015; Roth et al., 2012). Besides the potential paradigm shift in FH treatment, these findings imply that interfering with additional components of the LDLR degradation pathway (besides PCSK9) may provide alternative therapeutic avenues for hypercholesterolemia.

Despite the exciting developments with PCSK9 antibodies, a relevant caveat for further exploration of new therapies (new drugs or new formulations) for FH (and also other genetic liver diseases) is the lack of easily accessible and bona fide in vitro and in vivo models for preclinical testing. In vitro models for FH are mostly based on patient-derived hepatocytes from liver biopsy (Cayo et al., 2012), which have limited accessibility and cannot be expanded in culture. In vivo models including the hyperlipidemic rabbit, the rhesus macaque, and the *Ldlr* knockout mouse, have the limitation of not fully recapitulating human hepatocyte function (Bissig-Choisat et al., 2015). Patient-specific induced pluripotent stem cells (iPSCs) can provide an unlimited source of differentiated cell types including hepatocytes (iHeps) that can be used for in vitro and in vivo studies (Grskovic et al., 2011; Takahashi et al., 2007). This approach combined with the transplantation into immunodeficient mice may help overcome existing problems in modeling FH in vitro and in vivo (Carpentier et al., 2014; Chen et al., 2012; Liu et al., 2011). Several groups have generated FH iPSCs that harbor mutations in *LDLR* (Cayo et al., 2012; Ramakrishnan et al., 2015; Rashid et al., 2010) or *PCSK9* (Si-Tayeb et al., 2016) and have tested the ability of the derived iHeps to mimic the disease phenotype and respond to statins in vitro. However, there are no reports so far testing the effect of anti-PCSK9 therapies on FH iPSC-derived iHeps in vitro, or in vivo disease modeling and drug testing with FH iHeps transplanted into appropriate animal models.

Here, we report that FH iHeps derived from patient-specific and genetically engineered FH iPSCs can be used to test the efficacy of two well-known medications for lowering LDL-C, statins and PCSK9 antibodies, not only in vitro but also in vivo, by engrafting FH iHeps into the liver of immunodeficient mice knockout for *Ldlr*. With these assays, we have confirmed clinical observations of higher potency of PCSK9 antibodies compared with statins for treating FH (Robinson et al., 2015), indicating the potential of our model for further drug discovery and preclinical testing of experimental therapies.

RESULTS

Generation of a Panel of Patient-Specific and Genetically Engineered FH iPSCs for In Vitro and In Vivo Studies

We selected a family with clinical FH due to heterozygous duplication of "TGCTGGC" (c.2108_2114dup, p.Ala705fsX14) in exon 14 of *LDLR* (Khoo et al., 2000) (Figures 1A and 1B), which results in a premature stop codon. Using urinary cells as a donor cell source (Benda et al., 2013; Zhou et al., 2011) and episomal vectors as the reprogramming method (Yu et al., 2009), we generated integration-free iPSCs from the two affected sisters (FH-1 and FH-2) and the healthy sister (wild-type, WT) (Figures 1A and S1A); individual clones for each person were selected for further study. The resulting cell lines were fully pluripotent as shown by immunofluorescence (SSEA-4 and NANOG), RT-qPCR (*OCT4*, *SOX2*, *NANOG*, and *TERT*), DNA demethylation of the *NANOG* proximal promoter, and the formation of teratomas in immunocompromised mice (Figures S1B–S1E). Moreover, their karyotypes were normal (Figure S1C) and after serial passaging there was no remnant of the episomal vectors employed for reprogramming, as tested by PCR (Figure S1F). We also confirmed the *LDLR* mutation and the reduced expression of LDLR protein in the two FH iPSC clones by sequencing and western blotting, respectively (Figures 1B and 1C).

Next, because variations in the genetic background among iPSCs can be a confounding factor for in vitro disease modeling (Soldner et al., 2011), we used zinc-finger nucleases (ZFNs) (Moehle et al., 2007) targeting exon 4 of *LDLR* (Figure S2A) to create a panel of isogenic *LDLR* knockout iPSCs in a previously generated and well-characterized urinary iPSC clone from an unaffected individual (Zhou et al., 2011). This produced two biallelic knockout clones and 27 monoallelic knockout clones out of 214 clones screened by sequencing (Figure S2B). Of the resulting cell lines, we selected one monoallelic knockout (+/−) clone, one biallelic knockout (−/−) clone, and the unmodified control (+/+) as a panel for further study (Figure 1D). These isogenic iPSCs retained pluripotency, displayed normal karyotypes, and expressed LDLR levels according to their genotypes (Figures 1C, S2C, and S2D). Therefore, we have generated two complementary panels of iPSCs for studying FH mechanisms and performing drug screening.

PCSK9 Antibodies Show Stronger LDL-Lowering Ability than Statins in FH iHeps

We differentiated our panel of patient-specific and isogenic FH iPSCs into functional iHeps with a previously reported three-step protocol (Kajiwara et al., 2012). After 17 days of differentiation, iHeps with equivalent morphology to

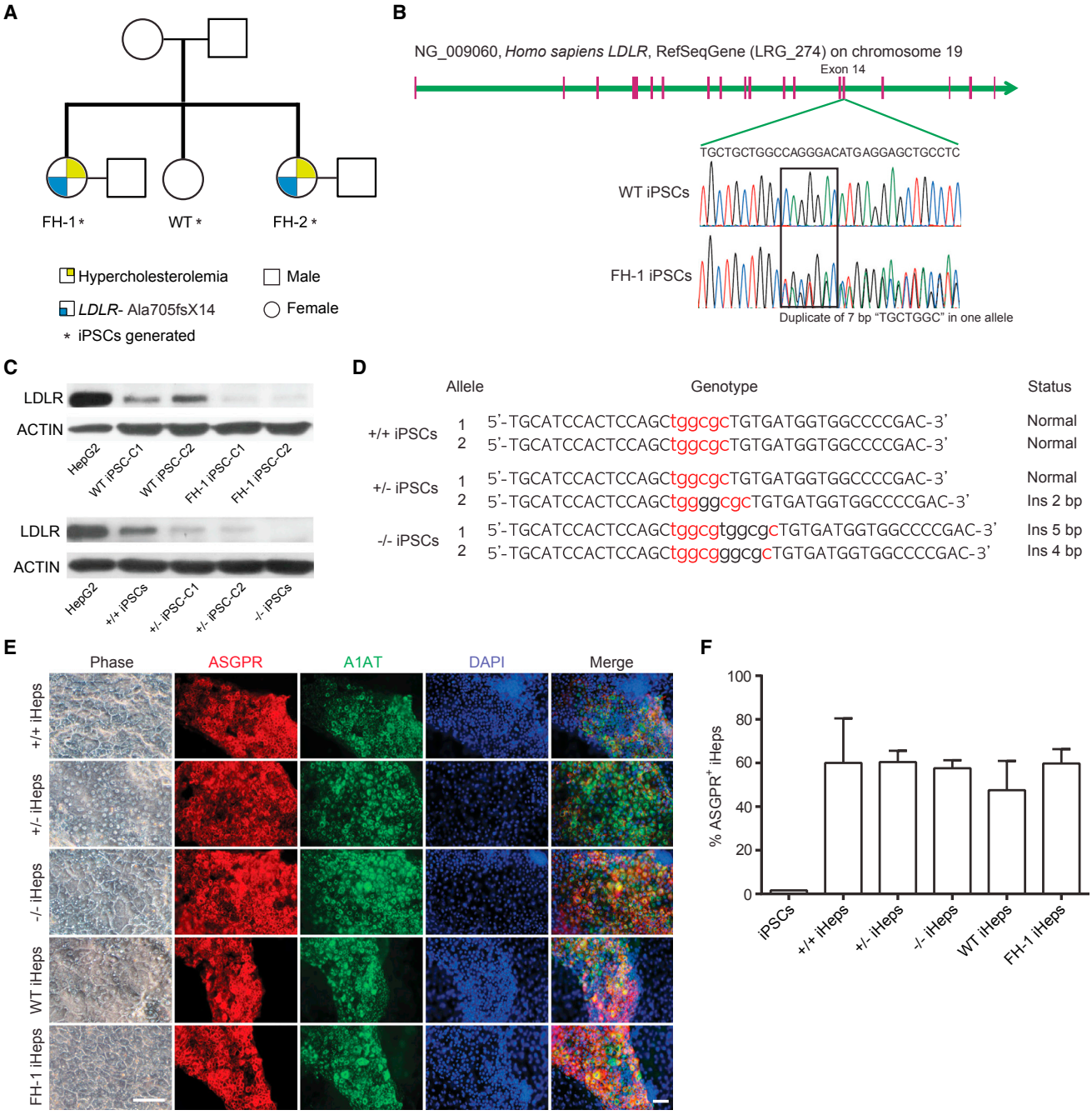

Figure 1. Generation of a Panel of FH iPSCs

(A) Family tree of WT and FH patients. Asterisk indicates patient-specific iPSCs generated in this study.

(B) Schematic depicting the genomic region of *LDLR* mutations in FH iPSCs. The boxed area indicates the position of heterozygous duplicate of "TGCTGGC" in FH-1 iPSCs.

(C) Western blotting shows LDLR levels in HepG2 cells (control) and iPSCs. ACTIN was used as loading control.

(D) Genotype of a panel of FH isogenic knockout iPSC clones. Red labels the interval of both ZFN-recognized fragments; black in lowercase among the red indicates insertion that resulted in frameshift.

(E) Phase contrast and immunofluorescence for ASGPR and A1AT of iHeps at day 17 of differentiation. Scale bars represent 50 μm.

(F) Bar graph shows the percentage of $ASGPR^{+}$ iHeps obtained with our differentiation protocol as measured by flow cytometry. A representative experiment with samples measured in triplicate is shown; error bars indicate SD.

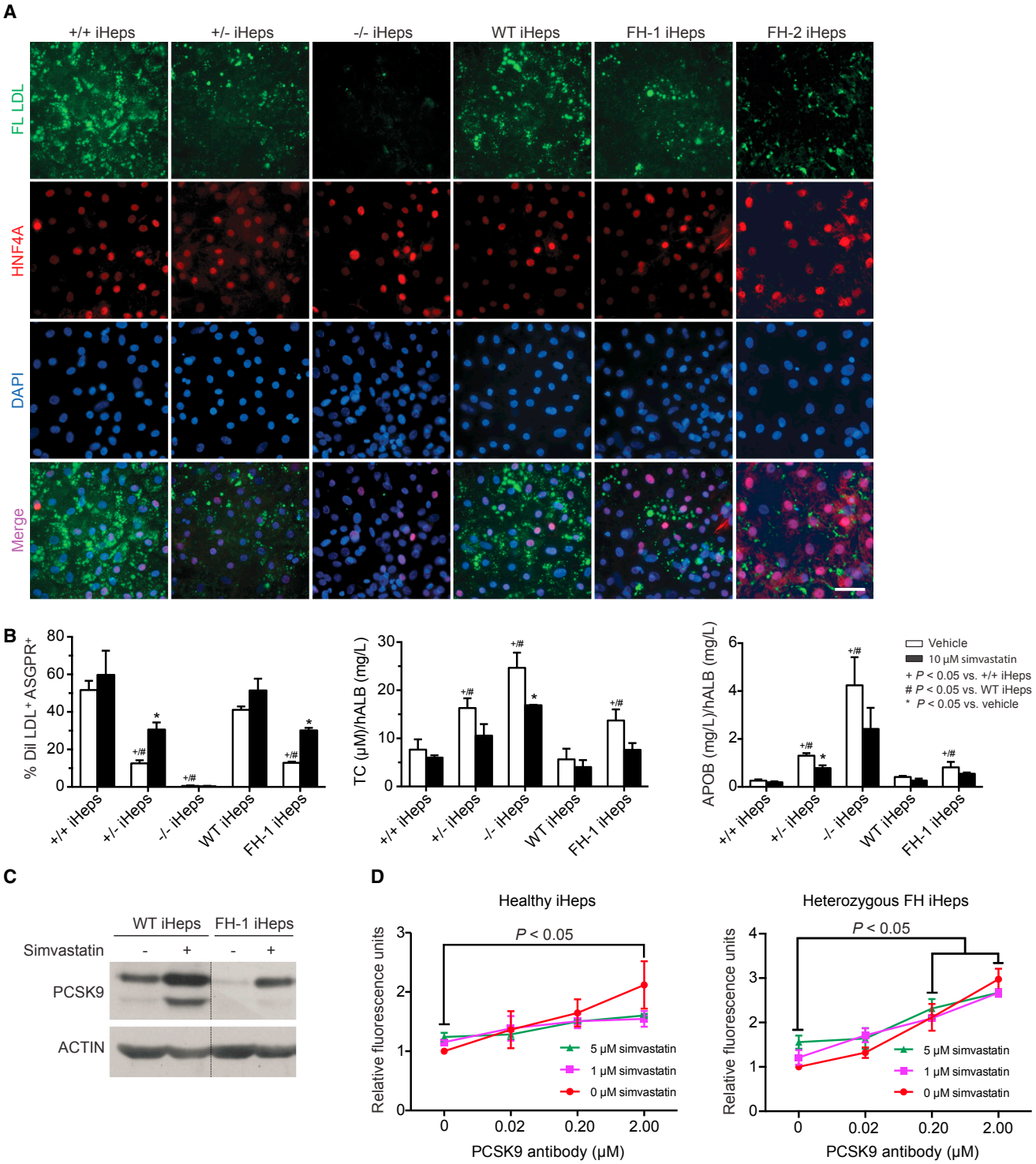

Figure 2. PCSK9 Antibodies Have a Stronger Effect than Statins on LDL Uptake by FH iHeps In Vitro

(A) Micrographs show co-localization of fluorescently labeled LDL (green) and HNF4A (red). Scale bars represent 50 μm.

(B) Left panel: bar graph shows percentage of DiI-LDL capture by flow cytometry in ASGPR$^+$ iHeps with or without simvastatin. Statistical tests were performed with three independent experiments; p values are indicated on the graph and were obtained using two-way ANOVA adjusted with Tukey's multiple comparison. Error bars indicate SEM. Middle and right panels: bar graphs show concentration of TC and APOB secretion in iHeps culture as determined by ELISA; values were normalized by the concentration of secreted hALB. Statistical tests were

(legend continued on next page)

human hepatocytes appeared (Figure 1E). These iHeps displayed markers of primary hepatocytes including asialoglycoprotein receptor (ASGPR) and α1-antitrypsin (A1AT) (Figure 1E), stored glycogen and lipids, secreted albumin and urea, and had the ability to metabolize rifampicin via the cytochrome P450 pathway (Figures S3A–S3E). Importantly, the efficiency of iHep differentiation between patient-specific and isogenic FH iPSCs was comparable, as measured by analyzing the population of $ASGPR^+$ cells by flow cytometry (Figure 1F).

To reveal the main phenotypic feature of FH (inability to uptake plasma LDL-C by hepatocytes) in vitro, we incubated iHeps from the various iPSC lines with 5 μg/mL fluorescently labeled LDL for 3.5 hr, followed by co-staining with hepatocyte nuclear factor 4α (HNF4A) to confirm the identity of the iHeps. As expected, WT and +/+ iHeps showed high—and rather comparable—LDL uptake while this was significantly impaired in FH-1, FH-2, and +/− iHeps, and completely abolished in −/− iHeps (Figure 2A). Similar results were obtained when LDL capture was measured using flow cytometry and normalized by the number of $ASGPR^+$ cells (Figure 2B, left panel). With the same assay, we also observed that 10 μM simvastatin elevated LDL uptake in FH-1 iHeps and +/− iHeps (Figure 2B, left panel), and more modestly in WT and +/+ iHeps. However, there was only marginal basal LDL uptake, without elevation with simvastatin, in −/− iHeps (Figure 2B, left panel). In addition, we measured total cholesterol (TC) and apolipoprotein B (APOB) secretion (an indirect measure of LDL secretion) (Cayo et al., 2012) in our panel of iHeps. TC and APOB were increased in FH-1 iHeps compared with WT, and in +/− and −/− iHeps compared with +/+ iHeps (Figure 2B, middle and right panels). On the other hand, 10 μM simvastatin reduced TC and APOB levels in iHeps from all tested iHeps but in particular in +/−, −/−, and FH-1 iHeps (Figure 2B, middle and right panels).

In the clinic, the inefficiency of statins in reducing LDL-C in some FH patients is partly due to increased PCSK9 expression, as this promotes LDLR degradation (Maxwell et al., 2005). To confirm whether PCSK9 is also upregulated by statins in iHeps in vitro, we performed western blotting of FH-1 and WT iHeps untreated or treated with simvastatin, observing that the treatment increases PCSK9 expression (Figure 2C). We then developed a 48-well-based assay to compare systematically the effect of different concentrations of statins and PCSK9 antibodies on LDL uptake in iHeps. In isolation, PCSK9 antibodies were more potent than simvastatin in inducing LDL uptake in healthy and heterozygous FH iHeps, and their combination did not increase it further (Figure 2D). Neither simvastatin nor PCSK9 antibodies had any effect on LDL uptake in −/− iHeps (Figure S3F). These in vitro results reproduce clinical observations showing that PCSK9 antibodies are a remarkable substitute for statins in treating heterozygous FH patients but are ineffective for homozygous FH patients (Stein et al., 2013).

Engrafted iHeps Reduce Plasma LDL-C Levels in an FH Chimeric Mouse Model

To further expand our iHep platform and perform drug testing in vivo, we crossed $Ldlr^{-/-}$ mice (Ishibashi et al., 1993) with $Rag2^{-/-}/Il2rg^{-/-}$ mice, and so generated triple-knockout *LRG* mice (Figure 3A). *LRG* mice lack an effective adaptive immune system, allowing the transplantation of human iHeps into an LDLR null background without rejection. To demonstrate this, we engrafted iHeps from FH iPSCs into *LRG* mice via intrasplenic injection. To improve the repopulation efficiency, we exposed mice to 3 Gy of γ-ray radiation 24 hr prior to engraftment to induce moderate liver injury and so enable proliferation of the engrafted iHeps. In addition, we suspended the injected iHeps in 50% Matrigel to provide a microenvironment that facilitates migration into the liver from the spleen (Figure 3B). The evidence of liver repopulation with iHeps in *LRG* mice was assessed by immunohistochemical staining for LDLR, human albumin (hALB), and human nuclear antigen (hNA) (Figures 3C and 3D). To determine iHep engraftment efficiency, we first stained chimeric mouse liver sections with hALB antibodies and then scanned the whole sections to quantify $hALB^+$ areas (Figures 3E, 3F, and S4A). With this strategy, we were able to assess iHep engraftment efficiency in multiple lobules and lobes rather than in small-area images. All tested iHeps showed significant repopulation in *LRG* mouse liver 3 weeks after transplantation, based on hALB staining, although with slight variations in efficiency (ranging from ∼5% to

performed on three independent experiments; p values are indicated on the graphs and were obtained using a Kruskal-Wallis test; error bars indicate SEM. Vehicle: DMSO.

(C) Western blotting shows that PCSK9 is induced by simvastatin in iHeps.

(D) LDL uptake capacity of healthy and heterozygous FH iHeps was measured with microplate readers and indicated as relative fluorescence units. Cells were treated with simvastatin and/or PCSK9 antibodies for 16 hr on days 17–21 of differentiation. Statistical tests were performed on three independent cell lines for both healthy (+/+, WT iHeps, and iHeps from another unaffected FH family member) and heterozygous FH iHeps (+/−, FH-1, and FH-2 iHeps). p Values are indicated on the figure and were obtained using one-way ANOVA adjusted with Dunnett's multiple comparison; error bars indicate SEM.

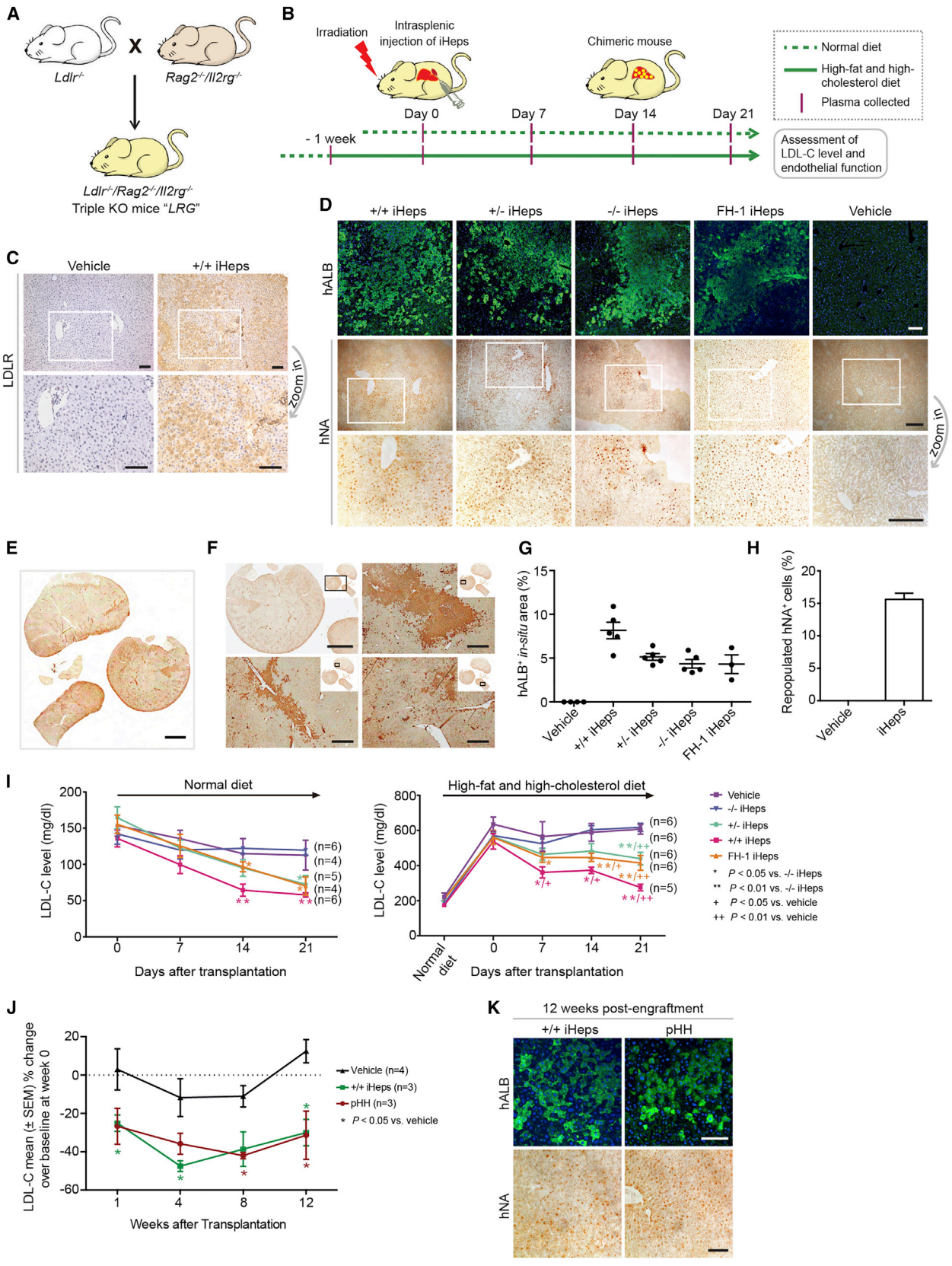

(legend on next page)

~10%) (Figure 3G). Because hALB is a secreted protein and dispersion could influence the assessment, we also used hNA to calculate iHep engraftment efficiency, which showed a moderately higher value than with hALB (~15% on average for different iHeps) (Figure 3H). No evidence of $hALB^+$ or hNA^+ cells was observed in *LRG* mouse liver engrafted with vehicle (Figures 3D and S4A). Likewise, there was no positive signal in the spleen of animals injected with iHeps (Figure S4B), demonstrating that transplanted cells do not engraft there after injection.

Fed a normal diet, *LRG* mice engrafted with +/+ iHeps had lower, but not statistically significant, levels of plasma LDL-C (n = 6, 57.9 ± 3.1 mg/dL) compared with vehicle (n = 4, 112.7 ± 20.6 mg/dL) 3 weeks after transplantation, while +/− iHeps (n = 4, 72.5 ± 12.0 mg/dL) and FH-1 iHeps (n = 5, 70.1 ± 12.7 mg/dL) were less effective (Figure 3I, left panel). As expected, −/− iHeps had no effect on LDL-C clearance (n = 6, 119.6 ± 6.9 mg/dL) compared with vehicle (Figure 3I, left panel). We then fed *LRG* mice with a high-fat, high-cholesterol (HFHC) diet to see whether this magnifies differences in LDL-C lowering after iHep transplantation. *LRG* mice showed around a 3-fold increase in LDL-C plasma after 1 week on HFHC diet (Figure 3I, right panel). Under this condition, transplanted +/+ iHeps (n = 5, 275.1 ± 19.0 mg/dL), and to a lesser extent +/− iHeps (n = 6, 439.3 ± 35.6 mg/dL) and FH-1 iHeps (n = 6, 414.7 ± 42.0 mg/dL), significantly downregulated plasma LDL-C levels compared with vehicle (n = 6, 606.7 ± 27.7 mg/dL) or −/− iHeps (n = 6, 617.3 ± 22.8 mg/dL) ($p < 0.01$, Figure 3I, right panel). To assess the long-term effects of engrafted iHeps compared with primary human hepatocytes (pHH), we tested LDL-C levels 12 weeks after transplantation of +/+ iHeps and pHH into *LRG* mice fed with HFHC diet, observing notable and rather comparable plasma LDL-C clearance in both cases compared with vehicle ($p < 0.05$, Figure 3J). The evidence of engrafted cells at this time point was assessed by staining for hALB and hNA in liver sections (Figure 3K). Overall, these experiments demonstrate that transplantation of LDLR-competent but not LDLR null iHeps promotes plasma LDL-C clearance in *LRG* mice.

Alirocumab Shows Stronger LDL-Lowering Ability than Statins in Chimeric *LRG* Mice

We then used HFHC diet to assess the effect of PCSK9 antibodies compared with statins on iHeps engrafted into *LRG* mice (Figure 4A). Importantly, we used a clinical-grade formulation of PCSK9 monoclonal antibodies, alirocumab (Sanofi and Regeneron Pharmaceuticals), which has completed phase III clinical trials (Robinson et al., 2015) and was approved by the Food and Drug Administration in July 2015 as a cholesterol-lowering drug. Alirocumab at 10 mg/kg/week enhanced plasma LDL-C clearance by engrafted +/− iHeps (Figure 4B; n = 3, percentage reduction from baseline 50.06% ± 7.38%, $p < 0.05$ compared with +/− iHeps alone) and FH-1 iHeps (Figure 4C; n = 3, percentage reduction from baseline 61.29% ± 10.80%, $p < 0.05$ compared with FH-1 iHeps alone) 21 days after treatment. Simvastatin at 10 mg/kg/day also reduced LDL-C clearance by engrafted +/− iHeps (n = 3, percentage reduction 33.37% ± 10.55%, $p > 0.05$ compared with iHeps alone) and FH-1 iHeps (n = 5, percentage reduction 28.39% ± 9.55%, $p > 0.05$ compared with iHeps alone), but less

Figure 3. Generation of Chimeric Mice Engrafted with FH iHeps

(A) Schematic view of derivation of *LRG* mice.

(B) Strategy for generation of FH chimeric mice, and assessment of LDL-C level and endothelial function.

(C and D) Immunohistochemical staining for LDLR, hNA, and hALB in *LRG* mouse liver repopulated with the indicated iHeps or Matrigel (vehicle). Zoomed images for LDLR and hNA are shown. Scale bars represent 50 μm (C) and 200 μm (D).

(E and F) Whole-slide scan image (E) and snapshot images (F) of hALB staining in mouse liver repopulated with +/+ iHeps. The location of snapshot images in the whole section is shown in the corner. Scale bars represent 2 mm (E and top left image in F) and 400 μm (remaining three images in F).

(G) Scatter diagram shows the percentage of engrafted $hALB^+$ iHeps in *LRG* mouse liver calculated based on whole-slide scanning images. Each dot represents one mouse with no less than four sections analyzed. Error bars indicate SEM.

(H) Bar graph shows the percentage of repopulated hNA^+ iHeps in *LRG* mouse liver (n = 4, including sections of *LRG* mice engrafted with +/+ iHeps × 1, +/− iHeps × 2, and −/− iHeps × 1); quantification of hNA^+ cells was performed by manual counting (see Supplemental Experimental Procedures for detailed description). Error bars indicate SEM.

(I) Plasma LDL-C levels in *LRG* mice engrafted with the indicated iHeps under normal diet (left panel) and HFHC diet (right panel) assessed at the indicated time points after iHep transplantation; n indicates number of mice. p Values are indicated on the figure and were obtained using a Kruskal-Wallis test; error bars indicate SEM.

(J) Percentage change of plasma LDL-C from baseline at weeks 1, 4, 8, and 12 post-transplantation in *LRG* mice fed with HFHC diet and engrafted with +/+ iHeps or pHH; n indicates number of mice. p Values are indicated on the figure and were obtained using a Kruskal-Wallis test; error bars indicate SEM.

(K) Immunohistochemical staining for hALB and hNA in *LRG* mouse liver repopulated with +/+ iHeps and pHH 12 weeks post-engraftment. Scale bars represent 200 μm.

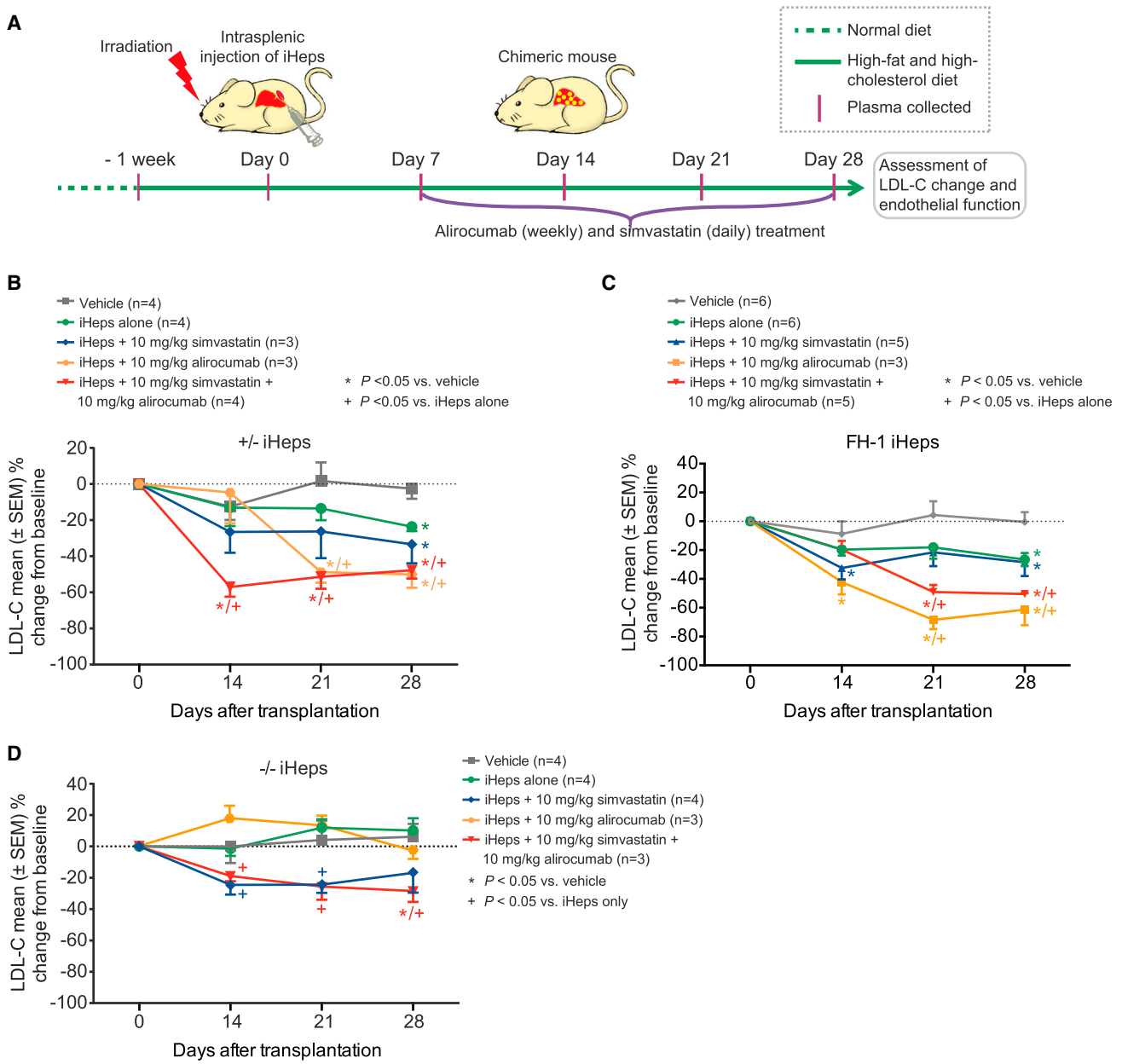

Figure 4. In Vivo Drug Testing with FH Chimeric Mice

(A) Strategy for in vivo drug testing using *LRG* mice engrafted with FH iHeps.

(B–D) Percentage change of plasma LDL-C from baseline at the indicated time points after iHep transplantation in *LRG* mice fed with HFHC diet and treated with simvastatin and/or PCSK9 antibodies; n indicates number of mice. p Values are indicated on the figure panel and were obtained using a Kruskal-Wallis test and error bars indicate SEM.

significantly than alirocumab, and their combination was not synergistic (Figures 4B and 4C). Moreover, in chimeric mice engrafted with −/− iHeps, alirocumab alone had no effect, while simvastatin alone or combined with alirocumab had only a modest effect on LDL-C clearance (Figure 4D). This moderate effect of simvastatin (alone or in combination) on engrafted −/− iHeps is likely due to inhibition of HMG-CoA reductase (Endo, 1992). Notably, the observed percentage reduction of plasma LDL-C with alirocumab in *LRG* mice engrafted with +/− iHeps or FH-1 iHeps is similar to that reported in human studies (Robinson et al., 2015; Roth et al., 2012). These results show the potential utility of *LRG* mice engrafted with FH iHeps for preclinical testing of novel drugs for FH.

Improvement of Endothelium-Dependent Vasodilation in Chimeric *LRG* Mice by Alirocumab and Statins

One consequence of FH is the accelerated development of atherosclerosis on the arterial wall (Vanhoutte et al., 2016), but we did not observe any obvious development of atherosclerotic lesions (assessed by oil red O staining) in our *LRG* mice fed with HFHC diet (data not shown). This is likely due to their compromised immune system and the relatively short period on the HFHC diet. Impaired endothelial function is an early indicator of atherosclerosis in children and young adults with FH (Wiegman et al., 2004), which manifests as reduced flow-mediated endothelium-dependent vasodilation (EDV) and increased proinflammatory gene expression, while EDV in response to glyceryl trinitrate in these patients is comparable with that in control subjects (Aggoun et al., 2000). We found that EDV induced by cumulative concentrations of acetylcholine (ACh) was significantly improved in aortic rings of *LRG* mice engrafted with +/+ iHeps compared with *LRG* mice engrafted with FH-1 iHeps, +/− iHeps, or −/− iHeps ($p < 0.01$, Figure 5A). However, endothelium-independent vasodilation induced by sodium nitroprusside was similar in endothelium-denuded aortic rings from all *LRG* groups (Figure 5B). Alirocumab at 10 mg/kg/week improved EDV significantly in *LRG* mice engrafted with +/− ($p < 0.01$) or FH-1 iHeps ($p < 0.05$, Figures 5C and 5D), while there was no effect on *LRG* mice engrafted with −/− iHeps or vehicle (Figures 5E and 5F). In contrast, 10 mg/kg/day simvastatin improved EDV in aortas of all groups (Figures 5C–5F), supporting the knowledge that the vasoprotective effect of simvastatin is partially independent of LDLR status (Tian et al., 2011). Moderate synergistic effect of simvastatin and alirocumab on EDV in aortic rings was observed in *LRG* mice engrafted with +/− iHeps or FH-1 iHeps, but not −/− iHeps or vehicle (Figures 5C–5F). Simvastatin or alirocumab did not have any effect on sodium nitroprusside-induced relaxation in aortic rings from *LRG* mice engrafted with all groups of iHeps or vehicle (Figures S5A–S5D). Furthermore, RT-qPCR of aorta samples from *LRG* mice engrafted with +/− iHeps showed that treatment with alirocumab, simvastatin, or their combination significantly reduced the expression of cytokines, chemokine receptors, and adhesion molecules related to vascular inflammation (Figure S5E). Therefore, EDV in aortas is a good readout for monitoring the consequences of FH in *LRG* mice engrafted with FH iHeps, and is responsive to treatment with PCSK9 antibodies or statins.

DISCUSSION

Patient-specific iPSCs can be differentiated into disease-relevant cells, thus providing an unlimited source of human cells for in vitro studies (Grskovic et al., 2011). Using this disease-in-a-dish approach, multiple human conditions including liver diseases have been modeled (Li et al., 2012; Rashid et al., 2010; Zhang et al., 2011). In this study, we have employed patient-specific FH iPSCs and genetically engineered isogenic FH iPSCs to create a platform for in vitro and in vivo drug testing of LDL-C-lowering therapies.

Several groups have previously reported FH iPSCs harboring mutations in *LDLR* and *PCSK9* and the ability of the derived iHeps to increase LDL uptake in vitro upon treatment with statins (Cayo et al., 2012; Ramakrishnan et al., 2015; Si-Tayeb et al., 2016). Our work has focused on testing therapies for FH, in particular anti-PCSK9 antibodies, in vitro and in vivo using FH iHeps, although this has been previously studied in vitro using pHH (Zhang et al., 2012). Likewise, FH disease modeling with isogenic iPSCs, which allow healthy versus diseased comparison of iHeps that share the same genetic background, had not been described beforehand. The addition of isogenic iPSCs may overcome the shortcomings of using a small number of patient-specific iPSCs and clones for identifying FH phenotypes in this study. Consistent with previous studies using FH iHeps (Cayo et al., 2012; Ramakrishnan et al., 2015; Si-Tayeb et al., 2016), our in vitro experiments confirm that statins increase LDL uptake in FH iHeps and also demonstrate a concomitant reduction in TC and APOB level. To facilitate the systematic screening of LDL-C-lowering medications with FH iHeps, we designed a 48-well assay based on labeled LDL capture. This assay showed higher efficacy in increasing LDL capture of PCSK9 antibodies compared with statins, and in the future may prove useful for identifying new candidate drugs for treating FH through systematic screening. In this regard, our assay may be adaptable to 96-well plates through further optimization.

Human liver chimeric mice carrying human pHH can facilitate in vivo study of viral hepatitis infections (Bissig et al., 2010; Carpentier et al., 2014) and liver genetic diseases (Bissig-Choisat et al., 2015; Yusa et al., 2011), and the testing of small molecular drug candidates and biological components including antibodies (Legrand et al., 2009). Embryonic stem cell (ESC)- or iPSC-derived iHeps have been used to generate chimeric mice by engrafting them into the liver of non-obese diabetic severe combined immunodeficient (NOD-SCID) mice (Chen et al., 2012), *NOD/Lt-SCID/IL-2Rγ*$^{-/-}$ (NSG) mice (Liu et al., 2011), or uPA transgenic mice (Basma et al., 2009; Carpentier et al., 2014), where iHeps showed further maturation and regeneration potential and displayed key activities of primary hepatocytes. Our study has produced a mouse model that lacks the gene (*Ldlr*) involved in a human disease (FH) and is engrafted with patient-specific iHeps to mimic the specific human disease condition and perform in vivo

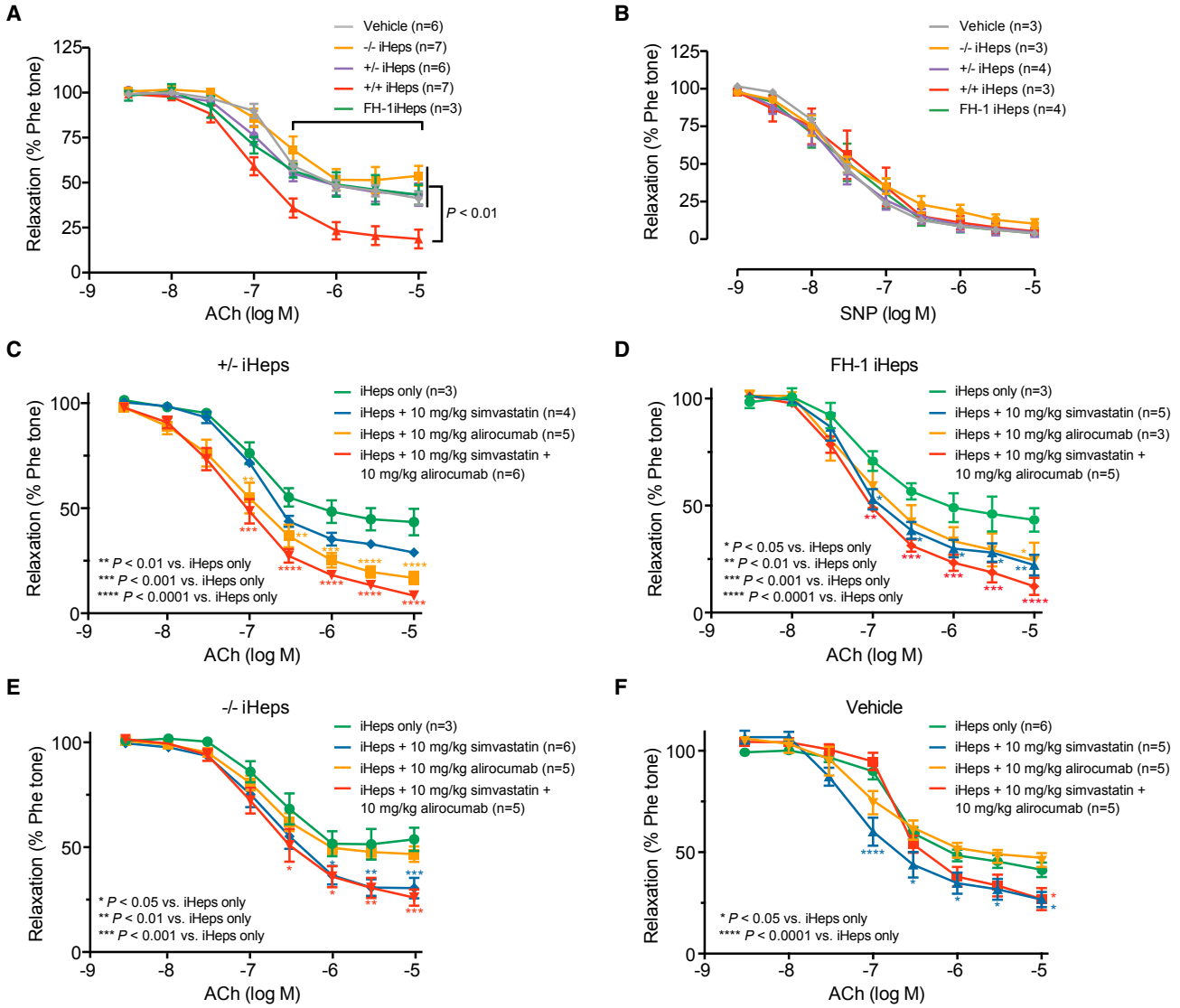

Figure 5. Alirocumab and Statins Improve EDV in Chimeric *LRG* Mice

(A and B) EDV in response to cumulative concentrations of acetylcholine (ACh) (A) and endothelium-independent vasodilation to sodium nitroprusside (SNP) (B) in aortas (precontracted with phentolamine [Phe]) from *LRG* mice fed with HFHC diet. Mice were engrafted with the indicated iHeps or vehicle; n indicates number of mice. p Values are indicated on the figure and were obtained using two-way ANOVA adjusted with Dunnett's multiple comparison; error bars indicate SEM.

(C–F) EDV in response to ACh in aortae (precontracted with Phe) from *LRG* mice fed with HFHC diet. Mice were engrafted with the indicated iHeps and treated with simvastatin (daily) and/or alirocumab (weekly); n indicates number of mice. p Values are indicated on the figure and were obtained using two-way ANOVA adjusted with Dunnett's multiple comparison; error bars indicate SEM.

drug testing. This approach has significant advantages over studies using *Ldlr* knockout mice alone (Ishibashi et al., 1993), as endogenous hepatocytes in the latter mouse model are not responsive to drugs modulating the LDLR pathway. A recent study showed engraftment of FH patient-specific iHeps injected subcutaneously rather than into the liver parenchyma of $Rag1^{-/-}/Ldlr^{-/-}$ mice, but the authors did not perform an assay to demonstrate functional recovery (Ramakrishnan et al., 2015). Another report demonstrated the feasibility of directly engrafting FH (due to compound heterozygosity in *LDLR* gene) pHH into $Fah^{-/-}/Rag2^{-/-}/Il2rg^{-/-}$ mice, and the phenotype of FH was successfully rescued by *LDLR* gene therapy using adeno-associated virus (Bissig-Choisat et al., 2015). Because of the lack of *Fah*, these mice had higher repopulation efficiency (>70%) (Bissig-Choisat et al., 2015) than our mice.

However, a problem of this approach is that a population of mouse hepatocytes with intact LDLR remains while the engrafted patients' pHH did not contain functional LDLR, which can be confounding factors when performing in vivo testing of drugs acting on the LDLR pathway. Moreover, primary FH hepatocytes are difficult to obtain and cannot be expanded in vitro. Although liver repopulation in our chimeric mice is significantly lower than for *Fah*$^{-/-}$/*Rag2*$^{-/-}$/*Il2rg*$^{-/-}$ mice engrafted with pHH (Azuma et al., 2007; Bissig-Choisat et al., 2015), it is comparable with results of recent reports describing NSG mice or Gunn rats (a model of Crigler-Najjar syndrome 1) engrafted with iPSC-derived iHeps (2%–17% [Liu et al., 2011] and 5.1% [Chen et al., 2015]). In the future, crossing our *LRG* mice with *Fah* knockout mice could help achieve higher liver chimerism, and thus further upgrade in vivo drug testing studies using engrafted FH iHeps. It should also be considered that mice and humans bear differences in lipoprotein metabolism, and therefore it may be desirable to genetically engineer other mammalian species (e.g., rabbits) (Shiomi and Ito, 2009) for more accurate studies using transplanted human FH iHeps. Nevertheless, despite the physiological differences between mice and humans and the moderate chimerism of our own model, the lowering of plasma LDL-C achieved with LDLR-competent iHeps was significant, while FH iHeps were less effective but exhibited good response to statins and particularly to PCSK9 antibodies. Besides plasma LDL-C levels, we measured endothelial function in aortas of *LRG* mice to assess the efficacy of engrafted iHeps and these two medications in vivo, as this parameter is affected early in patients with FH (Wiegman et al., 2004). Our results showed that cell therapy and the two medications could improve EDV in chimeric mice, indicating that endothelial function can be used as a parameter to evaluate disease progression during preclinical testing in chimeric *LRG* mice or other similar animal models. Importantly, we also noticed that the engrafted iHeps could be maintained in *LRG* mouse liver, and were functional, for at least 3 months. Overall, these results highlight the potential relevance of transplanting iPSC-derived iHeps for the treatment of hereditary metabolic liver disorders (Cantz et al., 2015), and the use of chimeric animals humanized with disease-specific iHeps for preclinical evaluation of novel therapies. However, the long-term therapeutic efficacy of iPSC-based approaches remains unclear, and future studies are necessary to address this as well as safety concerns.

In summary, our work provides a state-of-the-art in vitro and in vivo platform for testing drugs and experimental cell therapies using FH iHeps. Similar platforms using other gene knockout mice and alternative patient-specific iHeps may be useful to investigate pathological mechanisms and perform preclinical studies for unrelated inherited liver diseases.

EXPERIMENTAL PROCEDURES

DNA Sample Preparation and Sequencing

Genomic DNA was extracted from blood of subjects with FH using the QIAamp DNA blood kit (Qiagen). All exons of the *LDLR* gene locus were sequenced by Sanger sequencing, and mutations were identified by aligning with the reference sequence GenBank: NM_000527.4 from NCBI.

Cell Culture and Reprogramming

Urinary cells were obtained and expanded according to our published protocol (Zhou et al., 2012) with approval from the Institutional Review Board (HKCTR-725, http://www.hkclinicaltrials.com). Written informed consent from all patients is available upon request. Cells were reprogrammed with episomal vectors (Addgene) that encode human *OCT4*, *SOX2*, *KLF4*, *MYC*, *LIN28*, and *SV40LT* (Yu et al., 2009), using a previously reported protocol (Yu et al., 2011) with the combination of small molecular compounds containing 0.5 μM PD0325901 (Stemgent), 3 μM CHIR99021 (Stemgent), 0.5 μM A-83-01 (Stemgent), 1,000 U/mL human LIF (Millipore), 10 μM Y27632 (Sigma-Aldrich), and 100 ng/mL basic fibroblast growth factor (Peprotech). Human ESC-like colonies were picked at around day 25 and expanded in mTeSR1 (StemCell) on Matrigel (Corning)-coated plates with Accutase (Sigma-Aldrich).

Knockout Cell Line Generation

Sigma-Aldrich donated the *LDLR* ZFNs. *LDLR*-ZFN mRNAs were generated through in vitro transcription of *LDLR*-ZFN plasmids with a MessageMAX T7 ARCA-Capped Message Transcription Kit (Cambio) according to the manufacturer's specifications. The parental iPSC clone was reported previously (UC C0406-iPS C4) (Zhou et al., 2011). Detailed procedures are described in Supplemental Experimental Procedures.

In Vitro Differentiation of iPSCs into iHeps

Human iPSCs were differentiated into iHeps as reported previously (Kajiwara et al., 2012) but with small modifications at the endoderm induction stage: RPMI-1640 containing 100 ng/mL activin A (PeproTech) and 25 ng/mL WNT3a (R&D Systems) was employed for 1 day when the iPSCs had reached around 70% confluence, after which WNT3a was omitted from the medium for the following 2 days. HGF was purchased from PeproTech, Oncostatin M from R&D Systems, RPMI-1640, KnockOut DMEM, KnockOut Serum Replacement, and GlutaMAX Supplement from Life Technologies, DMSO from Sigma-Aldrich, and the HCM Bullet Kit from Lonza.

hALB, TC, and APOB Measurements

hALB, TC, and APOB measurements were performed on supernatants of day-17 to -18 (24-hr interval) iHeps culture by ELISA using a kit (Cell Biolabs for hALB and TC; MABTECH for APOB), in 96-well assay plates according to the manufacturer's specifications.

LDL Uptake Assays

LDL uptake assays employed fluorescently labeled LDL and 3,3′-dioctadecylindocarbocyanine (DiI)-LDL (Life Technologies), which were measured by microscopy or flow cytometry. Detailed procedures are described in Supplemental Experimental Procedures.

PCSK9 Antibodies and Simvastatin Treatments In Vitro

iPSCs were split onto 48-well plates and differentiated into iHeps as described above. At days 17–21 of differentiation, iHeps were treated with simvastatin and/or PCSK9 monoclonal antibodies (Cayman Chemical) for 16 hr and then incubated with 5 μg/mL DiI-LDL for 1 hr. Cells were washed with Ca^{2+}/Mg^{2+}-free PBS (CMF-PBS, Hyclone) and the DiI-LDL signal was captured with a CLARIOstar microplate reader (BMG LABTECH). Cells were then fixed with 4% paraformaldehyde and stained with ASGPR antibodies (Santa Cruz Biotechnology). Signal was read again with the microplate reader. Fluorescence signals were analyzed by MARS Data Analysis Software and normalized by the number of iHeps indicated by the ASGPR signal. Relative fluorescence units refer to the fold change of fluorescence values compared with the baseline (null treatment).

Chimeric Mice Generation

The animal study was approved by the Institutional Review Board (CULATR-2592-11 and 3003-13). *Ldlr*$^{-/-}$ mice (B6.129S7-*Ldlr*^{tm1Her}/J, The Jackson Laboratory) were crossed with *Rag2*$^{-/-}$/*Il2rg*$^{-/-}$ mice (available in our lab by crossing of B6(Cg)-*Rag2*$^{tm1.1Cgn}$/J mice with B6.129S4-*Il2rg*$^{tm1.wWjl}$/J mice purchased from The Jackson Laboratory) to generate *LRG* mice. Genotype was confirmed by PCR and sequencing using genomic DNA from mouse ear. As recipient for iHeps, we used 8- to 16-week-old *LRG* mice. Mice were irradiated with 3 Gy of γ-ray using a Gammacell 3000 Elan II (MDS Nordion) machine 24 hr prior to cell engraftment. A total of 10^6 iHeps or pHH (Lonza) suspended in 50 μL of 5.1 mg/mL Matrigel (Basement Membrane Matrix, Corning 354234) in CMF-PBS solution were engrafted into mouse liver by intrasplenic injection.

In Vivo Drug Testing

For the HFHC diet group, mice were fed with HFHC diet from 7 days prior to engraftment. For the drug treatment group, drugs were administered from 7 days post-engraftment. The clinical-grade PCSK9 monoclonal antibody formulation alirocumab (*SAR236553*/REGN727, Sanofi and Regeneron Pharmaceuticals) was injected subcutaneously (10 mg/kg/week) with or without simvastatin (Zocor; Merck Sharp & Dohme) treatment (10 mg/kg/day in drinking water) for 21 days. Blood samples were collected from the facial vein at the indicated time points and the day of engraftment of iHeps was set as day 0 or baseline. Plasma LDL-C level was evaluated using an L type LDL-C detection kit (Wako). Functional studies of EDV in response to ACh were performed in aortas precontracted with phentolamine using a myograph (Danish Myo Technology) as previously reported (Tian et al., 2011). Detailed procedures are described in Supplemental Experimental Procedures.

Statistical Analyses

Results are represented as the mean ± SEM unless otherwise indicated. Statistical analysis was performed with one-way or two-way ANOVA implemented in Prism 6 (version 6.03), or with Kruskal-Wallis test implemented in Scipy (version 0.18.1). All statistical tests were evaluated at a significance level of $p < 0.05$.

SUPPLEMENTAL INFORMATION

Supplemental Information includes Supplemental Experimental Procedures, five figures, and two tables and can be found with this article online at http://dx.doi.org/10.1016/j.stemcr.2017.01.027.

AUTHOR CONTRIBUTIONS

M.A.E. and H.-F.T. conceived the idea for this study and supervised the experiments. M.A.E. and H.-F.T. provided most of the funding. X.Z., B.Q., and X.B. contributed to the funding. J.Y., Y.W., T.Z., L.-Y.W., X.-Y.T., X.H., R.W., Y.L., L.-H.C., G.L., and Z.H. conducted the experiments. W.-H.L., K.-W.A., and A.P.H. provided technical support. W.F., P.Z., X.W., D.P.I., Z.L., Y.L., S.C., D.W, and L. Li provided materials or patient samples. X.Z., L. Lai, B.Q., X.B., Y.H., and C.-W.S. provided relevant advice. M.A.E., J.Y., and H.-F.T. analyzed the data and wrote the manuscript. M.A.E. and H.-F.T. approved the final version.

ACKNOWLEDGMENTS

We thank all members of our laboratories for their support. We also thank Jenny C.Y. Ho for her technical contribution to this work, Sigma-Aldrich for donation of *LDLR* ZFNs, and Sanofi and Regeneron Pharmaceuticals for providing PCSK9 antibodies (alirocumab). This work was supported by the Hong Kong Research Grant Council Theme Based Research Scheme (T12-705/11), The National Key Research and Development Program of China (2016YFA0100102), the Strategic Priority Research Program of the Chinese Academy of Sciences (XDA01020106), the Hong Kong Government Innovation and Technology Support Program (Tier 3) (ITS/303/12), the Cooperation Program of the Research Grants Council (RGC) of the Hong Kong Special Administrative Region and the National Natural Science Foundation of China (N-HKU 730/12 and 81261160506), the National Natural Science Foundation of China (8157050838 and 31370995), the Guangdong Province Science and Technology Program (2013B050800010, 2014A030312001, and 2016B030229007), the Guangzhou Science and Technology Cooperation Program (201508030027), the Shenzhen Science and Technology Council Basic Research program (JCYJ20150331142757383), the Pearl River Science and Technology Nova Program of Guangzhou (201610010107), and the Youth Innovation Promotion Association of the Chinese Academy of Sciences (2015294). H.-F.T. is the National Coordinator and Investigator of the ODYSSEY OUTCOMES study sponsored by Sanofi and Regeneron Pharmaceuticals.

Received: May 16, 2016
Revised: January 25, 2017
Accepted: January 26, 2017
Published: March 2, 2017

REFERENCES

Aggoun, Y., Bonnet, D., Sidi, D., Girardet, J.P., Brucker, E., Polak, M., Safar, M.E., and Levy, B.I. (2000). Arterial mechanical changes in children with familial hypercholesterolemia. Arterioscler. Thromb. Vasc. Biol. *20*, 2070–2075.

Azuma, H., Paulk, N., Ranade, A., Dorrell, C., Al-Dhalimy, M., Ellis, E., Strom, S., Kay, M.A., Finegold, M., and Grompe, M. (2007). Robust expansion of human hepatocytes in Fah(-/-)/Rag2(-/-)/Il2rg(-/-) mice. Nat. Biotechnol. *25*, 903–910.

Basma, H., Soto-Gutierrez, A., Yannam, G.R., Liu, L., Ito, R., Yamamoto, T., Ellis, E., Carson, S.D., Sato, S., Chen, Y., et al. (2009). Differentiation and transplantation of human embryonic stem cell-derived hepatocytes. Gastroenterology *136*, 990–999.

Benda, C., Zhou, T., Wang, X., Tian, W., Grillari, J., Tse, H.-F., Grillari-Voglauer, R., Pei, D., and Esteban, M.A. (2013). Urine as a source of stem cells. Adv. Biochem. Eng. Biotechnol. *129*, 19–32.

Bissig, K.D., Wieland, S.F., Tran, P., Isogawa, M., Le, T.T., Chisari, F.V., and Verma, I.M. (2010). Human liver chimeric mice provide a model for hepatitis B and C virus infection and treatment. J. Clin. Invest. *120*, 924–930.

Bissig-Choisat, B., Wang, L., Legras, X., Saha, P.K., Chen, L., Bell, P., Pankowicz, F.P., Hill, M.C., Barzi, M., Leyton, C.K., et al. (2015). Development and rescue of human familial hypercholesterolaemia in a xenograft mouse model. Nat. Commun. *6*, 7339.

Brown, M.S., and Goldstein, J.L. (1986). A receptor-mediated pathway for cholesterol homeostasis. Science *232*, 34–47.

Cannon, C.P., Blazing, M.A., Giugliano, R.P., McCagg, A., White, J.A., Theroux, P., Darius, H., Lewis, B.S., Ophuis, T.O., Jukema, J.W., et al. (2015). Ezetimibe added to statin therapy after acute coronary syndromes. N. Engl. J. Med. *372*, 2387–2397.

Cantz, T., Sharma, A.D., and Ott, M. (2015). Concise review: cell therapies for hereditary metabolic liver diseases-concepts, clinical results, and future developments. Stem Cells *33*, 1055–1062.

Carpentier, A., Tesfaye, A., Chu, V., Nimgaonkar, I., Zhang, F., Lee, S.B., Thorgeirsson, S.S., Feinstone, S.M., and Liang, T.J. (2014). Engrafted human stem cell-derived hepatocytes establish an infectious HCV murine model. J. Clin. Invest. *124*, 4953–4964.

Cayo, M.A., Cai, J., DeLaForest, A., Noto, F.K., Nagaoka, M., Clark, B.S., Collery, R.F., Si-Tayeb, K., and Duncan, S.A. (2012). JD induced pluripotent stem cell–derived hepatocytes faithfully recapitulate the pathophysiology of familial hypercholesterolemia. Hepatology *56*, 2163–2171.

Chen, Y.F., Tseng, C.Y., Wang, H.W., Kuo, H.C., Yang, V.W., and Lee, O.K. (2012). Rapid generation of mature hepatocyte-like cells from human induced pluripotent stem cells by an efficient three-step protocol. Hepatology *55*, 1193–1203.

Chen, Y., Li, Y.F., Wang, X., Zhang, W., Sauer, V., Chang, C.J., Han, B., Tchaikovskaya, T., Avsar, Y., Tafaleng, E., et al. (2015). Amelioration of hyperbilirubinemia in Gunn rats after transplantation of human induced pluripotent stem cell-derived hepatocytes. Stem Cell Rep. *5*, 22–30.

Dormuth, C.R., Filion, K.B., Paterson, J.M., James, M.T., Teare, G.F., Raymond, C.B., Rahme, E., Tamim, H., and Lipscombe, L. (2014). Higher potency statins and the risk of new diabetes: multicentre, observational study of administrative databases. BMJ *348*, g3244.

Dubuc, G., Chamberland, A., Wassef, H., Davignon, J., Seidah, N.G., Bernier, L., and Prat, A. (2004). Statins upregulate PCSK9, the gene encoding the proprotein convertase neural apoptosis-regulated convertase-1 implicated in familial hypercholesterolemia. Arterioscler. Thromb. Vasc. Biol. *24*, 1454–1459.

Endo, A. (1992). The discovery and development of HMG-CoA reductase inhibitors. J. Lipid. Res. *33*, 1569–1582.

Grskovic, M., Javaherian, A., Strulovici, B., and Daley, G.Q. (2011). Induced pluripotent stem cells—opportunities for disease modelling and drug discovery. Nat. Rev. Drug Discov. *10*, 915–929.

Ishibashi, S., Brown, M.S., Goldstein, J.L., Gerard, R.D., Hammer, R.E., and Herz, J. (1993). Hypercholesterolemia in low density lipoprotein receptor knockout mice and its reversal by adenovirus-mediated gene delivery. J. Clin. Invest. *92*, 883–893.

Kajiwara, M., Aoi, T., Okita, K., Takahashi, R., Inoue, H., Takayama, N., Endo, H., Eto, K., Toguchida, J., Uemoto, S., et al. (2012). Donor-dependent variations in hepatic differentiation from human-induced pluripotent stem cells. Proc. Natl. Acad. Sci. USA *109*, 12538–12543.

Khoo, K.L., van Acker, P., Defesche, J.C., Tan, H., van de Kerkhof, L., Heijnen-van Eijk, S.J., Kastelein, J.J., and Deslypere, J.P. (2000). Low-density lipoprotein receptor gene mutations in a Southeast Asian population with familial hypercholesterolemia. Clin. Genet. *58*, 98–105.

Legrand, N., Ploss, A., Balling, R., Becker, P.D., Borsotti, C., Brezillon, N., Debarry, J., de Jong, Y., Deng, H.K., Di Santo, J.P., et al. (2009). Humanized mice for modeling human infectious disease: challenges, progress, and outlook. Cell Host Microbe *6*, 5–9.

Li, W., Wang, X., Fan, W., Zhao, P., Chan, Y.C., Chen, S., Zhang, S., Guo, X., Zhang, Y., Li, Y., et al. (2012). Modeling abnormal early development with induced pluripotent stem cells from aneuploid syndromes. Hum. Mol. Genet. *21*, 32–45.

Liu, H., Kim, Y., Sharkis, S., Marchionni, L., and Jang, Y.Y. (2011). In vivo liver regeneration potential of human induced pluripotent stem cells from diverse origins. Sci. Transl. Med. *3*, 82ra39.

Maxwell, K.N., Fisher, E.A., and Breslow, J.L. (2005). Overexpression of PCSK9 accelerates the degradation of the LDLR in a post-endoplasmic reticulum compartment. Proc. Natl. Acad. Sci. USA *102*, 2069–2074.

Moehle, E.A., Rock, J.M., Lee, Y.-L., Jouvenot, Y., DeKelver, R.C., Gregory, P.D., Urnov, F.D., and Holmes, M.C. (2007). Targeted gene addition into a specified location in the human genome using designed zinc finger nucleases. Proc. Natl. Acad. Sci. USA *104*, 3055–3060.

Ramakrishnan, V.M., Yang, J.Y., Tien, K.T., McKinley, T.R., Bocard, B.R., Maijub, J.G., Burchell, P.O., Williams, S.K., Morris, M.E., Hoying, J.B., et al. (2015). Restoration of physiologically responsive low-density lipoprotein receptor-mediated endocytosis in genetically deficient induced pluripotent stem cells. Sci. Rep. *5*, 13231.

Rashid, S.T., Corbineau, S., Hannan, N., Marciniak, S.J., Miranda, E., Alexander, G., Huang-Doran, I., Griffin, J., Ahrlund-Richter, L., Skepper, J., et al. (2010). Modeling inherited metabolic disorders

of the liver using human induced pluripotent stem cells. J. Clin. Invest. *120*, 3127–3136.

Reiner, Z. (2015). Management of patients with familial hypercholesterolaemia. Nat. Rev. Cardiol. *12*, 565–575.

Robinson, J.G., Farnier, M., Krempf, M., Bergeron, J., Luc, G., Averna, M., Stroes, E.S., Langslet, G., Raal, F.J., and El Shahawy, M. (2015). Efficacy and safety of alirocumab in reducing lipids and cardiovascular events. N. Engl. J. Med. *372*, 1489–1499.

Roth, E.M., McKenney, J.M., Hanotin, C., Asset, G., and Stein, E.A. (2012). Atorvastatin with or without an antibody to PCSK9 in primary hypercholesterolemia. N. Engl. J. Med. *367*, 1891–1900.

Shiomi, M., and Ito, T. (2009). The Watanabe heritable hyperlipidemic (WHHL) rabbit, its characteristics and history of development: a tribute to the late Dr. Yoshio Watanabe. Atherosclerosis *207*, 1–7.

Si-Tayeb, K., Idriss, S., Champon, B., Caillaud, A., Pichelin, M., Arnaud, L., Lemarchand, P., Le May, C., Zibara, K., and Cariou, B. (2016). Urine-sample-derived human induced pluripotent stem cells as a model to study PCSK9-mediated autosomal dominant hypercholesterolemia. Dis. Model. Mech. *9*, 81–90.

Sniderman, A.D., Tsimikas, S., and Fazio, S. (2014). The severe hypercholesterolemia phenotype: clinical diagnosis, management, and emerging therapies. J. Am. Coll. Cardiol. *63*, 1935–1947.

Soldner, F., Laganière, J., Cheng, A.W., Hockemeyer, D., Gao, Q., Alagappan, R., Khurana, V., Golbe, L.I., Myers, R.H., and Lindquist, S. (2011). Generation of isogenic pluripotent stem cells differing exclusively at two early onset Parkinson point mutations. Cell *146*, 318–331.

Stein, E.A., Honarpour, N., Wasserman, S.M., Xu, F., Scott, R., and Raal, F.J. (2013). Effect of the PCSK9 monoclonal antibody, AMG 145, in homozygous familial hypercholesterolemia. Circulation *128*, 2113–2120.

Stroes, E.S., Thompson, P.D., Corsini, A., Vladutiu, G.D., Raal, F.J., Ray, K.K., Roden, M., Stein, E., Tokgozoglu, L., Nordestgaard, B.G., et al. (2015). Statin-associated muscle symptoms: impact on statin therapy—European Atherosclerosis Society consensus panel statement on assessment, aetiology and management. Eur. Heart J. *36*, 1012–1022.

Takahashi, K., Tanabe, K., Ohnuki, M., Narita, M., Ichisaka, T., Tomoda, K., and Yamanaka, S. (2007). Induction of pluripotent stem cells from adult human fibroblasts by defined factors. Cell *131*, 861–872.

Tian, X.Y., Wong, W.T., Xu, A., Chen, Z.Y., Lu, Y., Liu, L.M., Lee, V.W., Lau, C.W., Yao, X., and Huang, Y. (2011). Rosuvastatin improves endothelial function in db/db mice: role of angiotensin II type 1 receptors and oxidative stress. Br. J. Pharmacol. *164*, 598–606.

Vanhoutte, P.M., Zhao, Y., Xu, A., and Leung, S.W. (2016). Thirty years of saying NO: sources, fate, actions, and misfortunes of the endothelium-derived vasodilator mediator. Circ. Res. *119*, 375–396.

Wiegman, A., Hutten, B.A., de Groot, E., Rodenburg, J., Bakker, H.D., Buller, H.R., Sijbrands, E.J., and Kastelein, J.J. (2004). Efficacy and safety of statin therapy in children with familial hypercholesterolemia: a randomized controlled trial. JAMA *292*, 331–337.

Yu, J., Hu, K., Smuga-Otto, K., Tian, S., Stewart, R., Slukvin, I.I., and Thomson, J.A. (2009). Human induced pluripotent stem cells free of vector and transgene sequences. Science *324*, 797–801.

Yu, J., Chau, K.F., Vodyanik, M.A., Jiang, J., and Jiang, Y. (2011). Efficient feeder-free episomal reprogramming with small molecules. PLoS One *6*, e17557.

Yusa, K., Rashid, S.T., Strick-Marchand, H., Varela, I., Liu, P.Q., Paschon, D.E., Miranda, E., Ordonez, A., Hannan, N.R., Rouhani, F.J., et al. (2011). Targeted gene correction of alpha1-antitrypsin deficiency in induced pluripotent stem cells. Nature *478*, 391–394.

Zhang, S., Chen, S., Li, W., Guo, X., Zhao, P., Xu, J., Chen, Y., Pan, Q., Liu, X., Zychlinski, D., et al. (2011). Rescue of ATP7B function in hepatocyte-like cells from Wilson's disease induced pluripotent stem cells using gene therapy or the chaperone drug curcumin. Hum. Mol. Genet. *20*, 3176–3187.

Zhang, L.W., McCabe, T., Condra, J.H., Ni, Y.G., Peterson, L.B., Wang, W.R., Strack, A.M., Wang, F.B., Pandit, S., Hammond, H., et al. (2012). An anti-PCSK9 antibody reduces LDL-cholesterol on top of a statin and suppresses hepatocyte SREBP-regulated genes. Int. J. Biol. Sci. *8*, 310–327.

Zhou, T., Benda, C., Duzinger, S., Huang, Y., Li, X., Li, Y., Guo, X., Cao, G., Chen, S., and Hao, L. (2011). Generation of induced pluripotent stem cells from urine. J. Am. Soc. Nephrol. *22*, 1221–1228.

Zhou, T., Benda, C., Dunzinger, S., Huang, Y., Ho, J.C., Yang, J., Wang, Y., Zhang, Y., Zhuang, Q., and Li, Y. (2012). Generation of human induced pluripotent stem cells from urine samples. Nat. Protoc. *7*, 2080–2089.

Stem Cell Reports, Volume *8*

Supplemental Information

Generation of Human Liver Chimeric Mice with Hepatocytes from Familial Hypercholesterolemia Induced Pluripotent Stem Cells

Jiayin Yang, Yu Wang, Ting Zhou, Lai-Yung Wong, Xiao-Yu Tian, Xueyu Hong, Wing-Hon Lai, Ka-Wing Au, Rui Wei, Yuqing Liu, Lai-Hung Cheng, Guichan Liang, Zhijian Huang, Wenxia Fan, Ping Zhao, Xiwei Wang, David P. Ibañez, Zhiwei Luo, Yingying Li, Xiaofen Zhong, Shuhan Chen, Dongye Wang, Li Li, Liangxue Lai, Baoming Qin, Xichen Bao, Andrew P. Hutchins, Chung-Wah Siu, Yu Huang, Miguel A. Esteban, and Hung-Fat Tse

Supplemental Figure S1

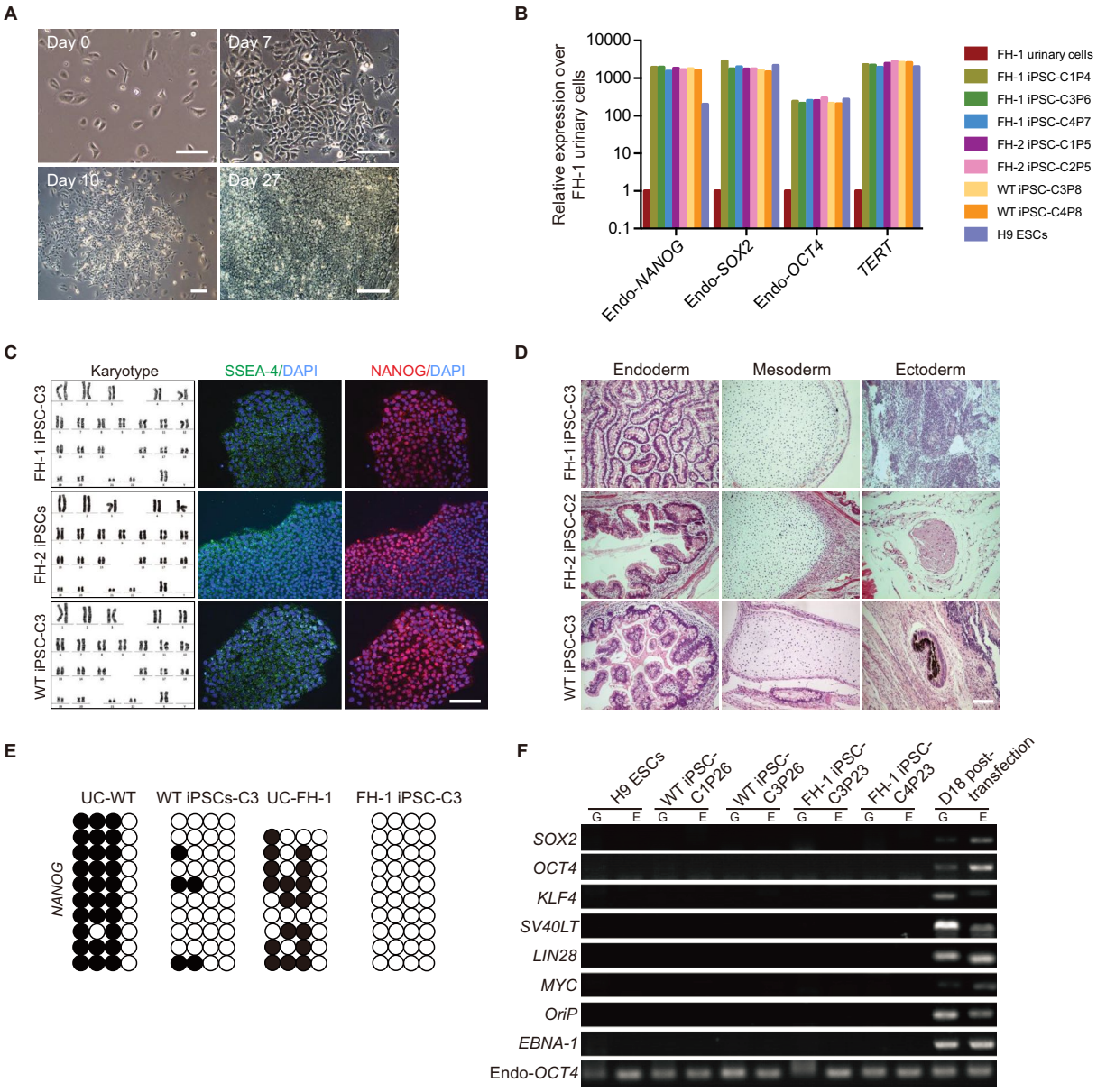

Supplemental Figure S1. Generation of Footprint-Free Patient-Specific iPSCs with Episomal Vectors. Related to Figure 1. A, Representative phase contrast images of different time points of episomal vector-mediated reprogramming, urinary cells were transfected with vectors at day 0. Scale bars represent 200 μm. **B**, RT-qPCR for endogenous (Endo-) *NANOG, OCT4, SOX2*, and *TERT* in the indicated iPSCs. H9 ESCs were used as control, values are referred to non-transfected FH-1 urinary cells. **C**, Phase contrast images of karyotype analysis (1^{st} column) and representative immunofluorescence microscopy photographs for SSEA-4 and NANOG (2^{nd} and 3^{rd} column) of the indicated iPSCs. Scale bars represent 100 μm. **D,** Representative images of hematoxylin/eosin stained sections of teratomas generated by injecting the indicated iPSCs into SCID mice. Scale bars represent 100 μm. **E,** DNA methylation profile of the *NANOG* proximal promoter for the indicated cell types. UC: urinary cells. **F**, Residual and random integration test of episomal DNA in the indicated iPSCs using PCR. G: genomic DNA. E: episomal DNA. Genomic DNA from H9 ESCs and urinary cells transfected with episomal vectors (day 18 post-transfection) were used as negative and positive controls, respectively.

Supplemental Figure S2

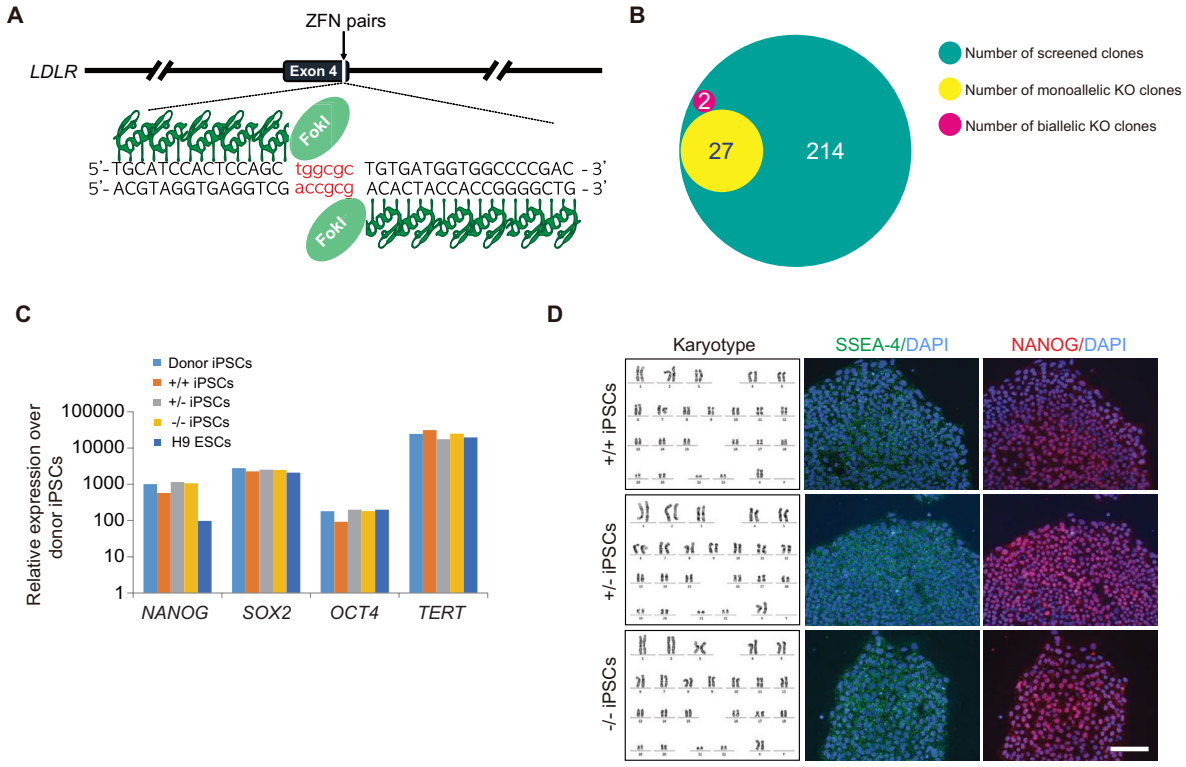

Supplemental Figure S2. Generation of Monoallelic and Biallelic *LDLR* Knockout iPSCs with ZFNs. Related to Figure 1. A, Schematic of the *LDLR* coding region depicting the genomic locus targeted by *LDLR*-ZFNs. **B,** Summary of genome editing experiments with ZFNs and numbers of analyzed subclones. Among a total number of 214 clones screened, 2 were biallelic knockout and 27 were monoallelic knockout. **C**, RT-qPCR for endogenous *NANOG, OCT4, SOX2*, and *TERT* in the indicated iPSCs. H9 ESCs were used as control, values are referred to non-transfected urinary cells. **D**, Phase contrast images of karyotype analysis (1st column), and representative immunofluorescence microscopy photographs for SSEA-4 and NANOG (2nd and 3rd column) of the indicated iPSCs. Scale bars represent 100 μm.

Supplemental Figure S3

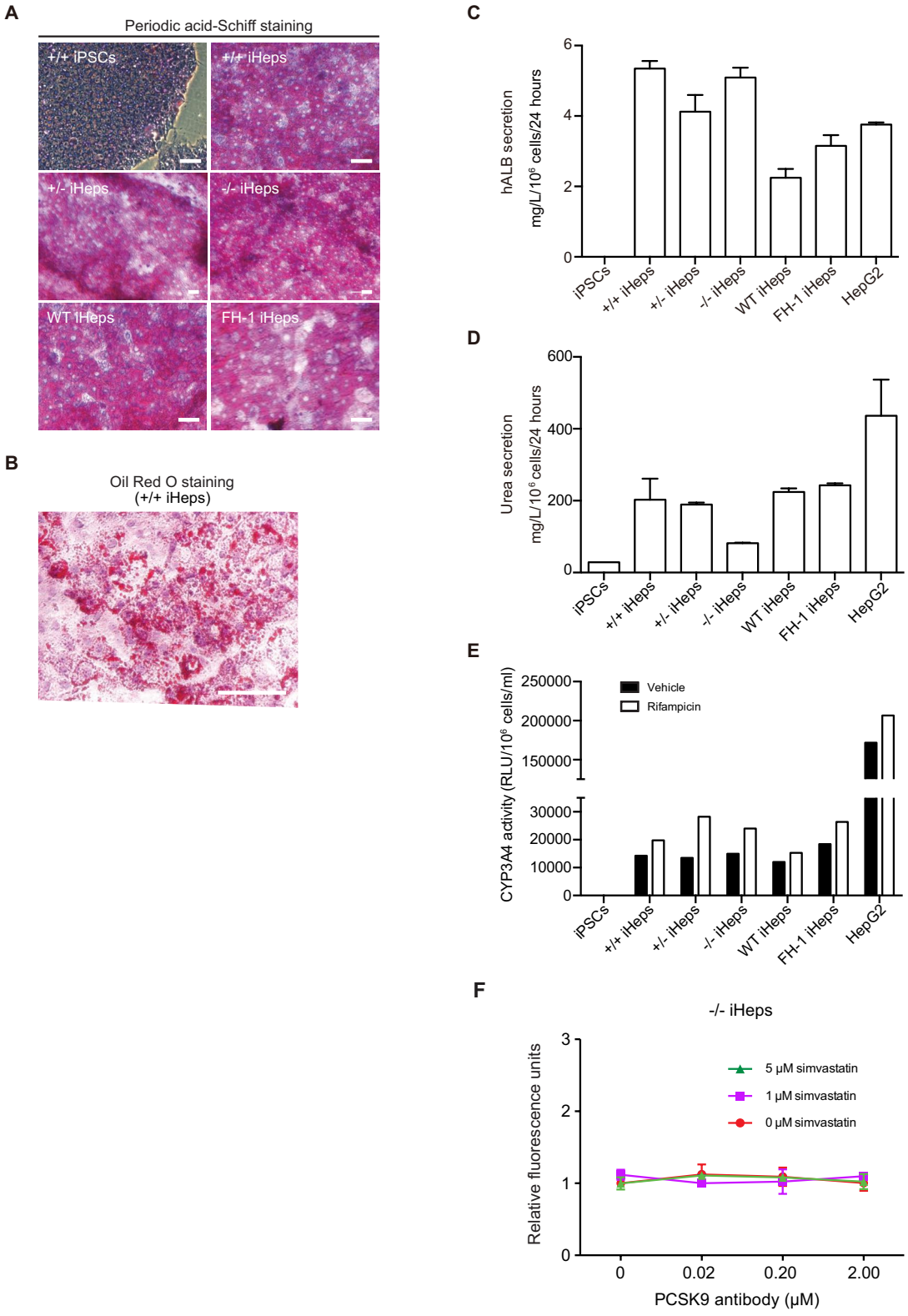

Supplemental Figure S3. Characterization of iHeps. Related to Figure 2. A, Representative images of PAS staining for the indicated iPSC-derived iHeps at day 17 of differentiation. Scale bars represent 50 μm. **B**, Representative images of oil red O staining in +/+ iHeps. Scale bar represents 100 μm. **C**, Bar graph shows hALB secretion level (mg/L/10^6 cells/24 hours) in the indicated iHeps. HepG2 cells and iPSCs were used as positive and negative controls, respectively (also in D and E). A representative experiment with samples measured in triplicate is shown; error bars indicate SD. **D**, Bar graph shows urea secretion (mg/L/10^6 cells/24 hours) in the indicated iHeps. A representative experiment with samples measured in duplicate is shown; error bars indicate SD. **E**, Detection of cytochrome P450 (CYP3A4) metabolic activity (RLU/10^6 cells/ml) of iHeps at day 20 of differentiation after 72 hours of rifampicin induction compared to vehicle. **F,** LDL uptake capacity of -/- iHeps measured with a microplate reader and indicated as relative fluorescence units. Cells were treated with simvastatin and/or PCSK9 antibodies for 16 hours on day 17-21 of differentiation. A representative experiment with samples measured in at least duplicate is shown, error bars indicate SEM.

Supplemental Figure S4

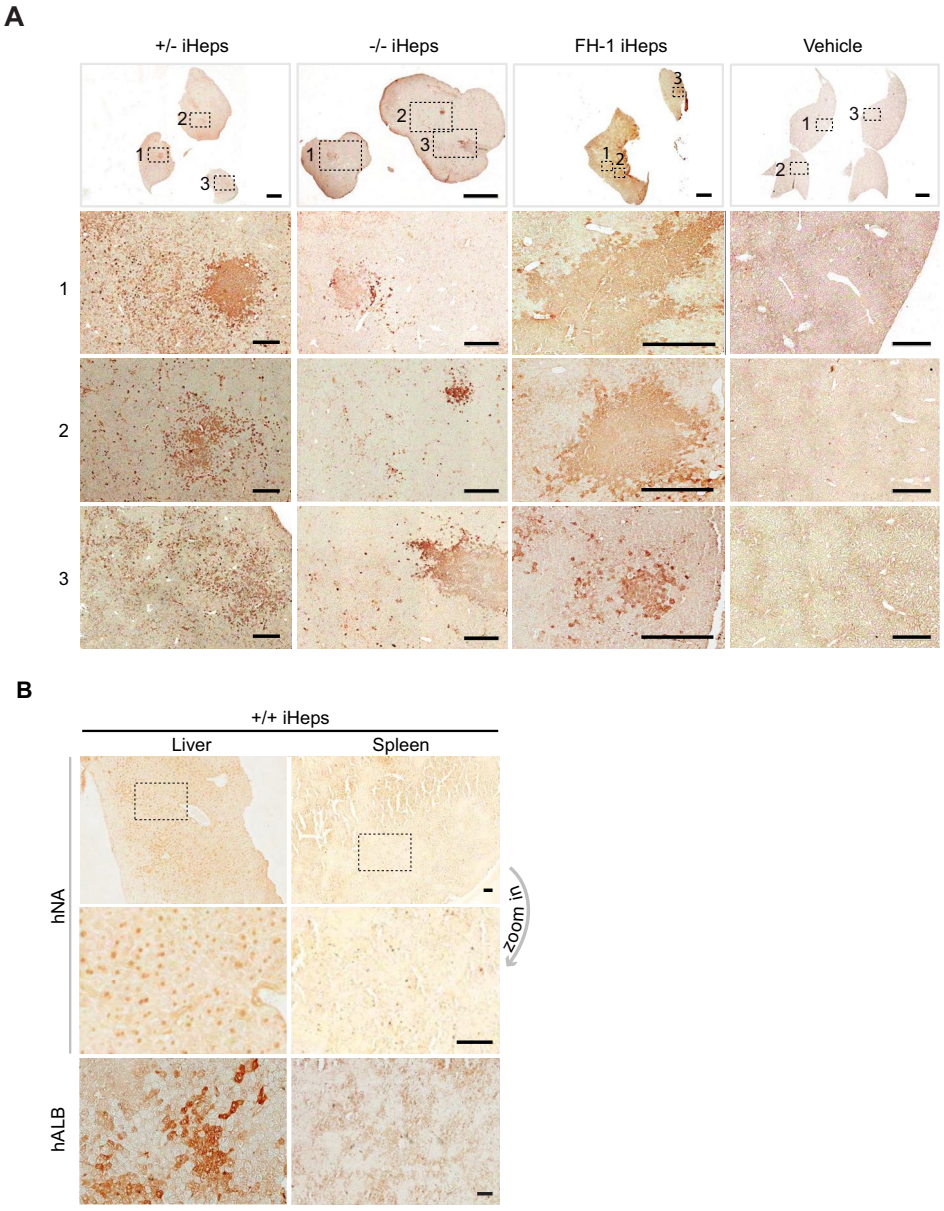

Supplemental Figure S4. iHeps Repopulate *LRG* Mice Liver. Related to Figure 3. A, Top panel, whole-slide scan images of hALB (brown) staining in chimeric mice liver repopulated with the indicated iHeps or vehicle. Scale bars represent 2 mm. Lower panels, zoomed hALB+ areas of the scanned sections are shown as indexed. Scale bars represent 400 μm. **B,** Immunohistochemical staining for hNA (brown) and hALB (brown) in the liver and spleen of *LRG* mice engrafted with +/+ iHeps. Zoomed images for hNA are also shown. Scale bars represent 50 μm.

Supplemental Figure S5

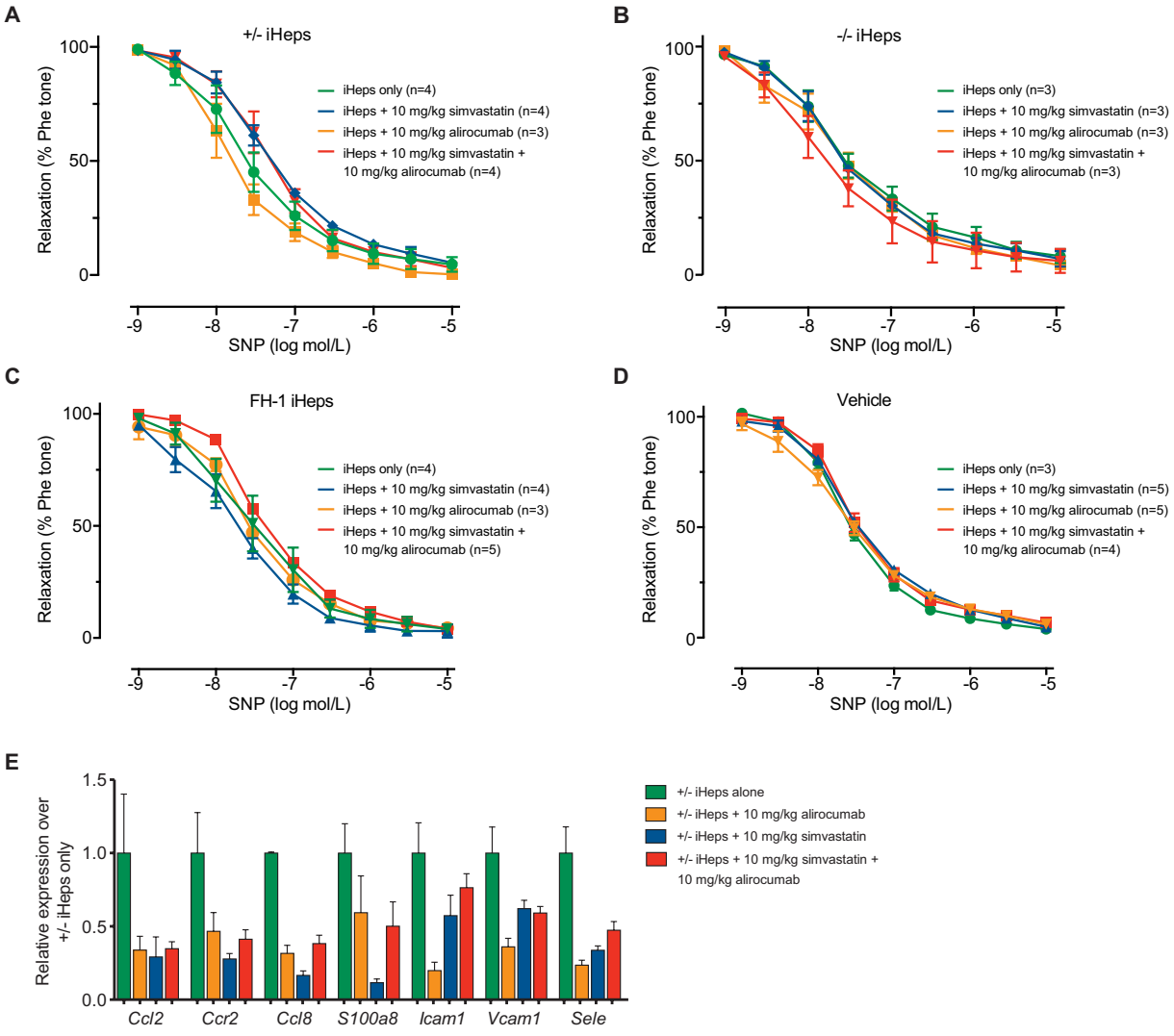

Supplemental Figure S5. Measurement of Endothelium-Independent Vasodilation and Expression of Proinflammatory Markers upon Alirocumab and Simvastatin Treatment. Related to Figure 5. A-D, Endothelium-independent vasodilation in response to SNP in aortae (pre-contracted with Phe) from *LRG* mice fed with HFHC diet. Mice were engrafted with the indicated iHeps or vehicle, and treated with simvastatin (daily) and/or alirocumab (weekly); n indicates number of mice. **E,** RT-qPCR of aortae from *LRG* mice engrafted with +/- iHeps shows the level of gene expression for the indicated cytokines, chemokine receptors, and adhesion molecules related to vascular inflammation.

Supplemental Table S1

List of Primers Used in this Study

RT-qPCR primers for human endogenous pluripotent genes		
Gene	Sequence (5'→3')	
ACTB	Forward	CCCAGAGCAAGAGAGG
	Reverse	GTCCAGACGCAGGATG
NANOG	Forward	TGAACCTCAGCTACAAACAG
	Reverse	TGGTGGTAGGAAGAGTAAAG
OCT4	Forward	CCTCACTTCACTGCACTGTA
	Reverse	CAGGTTTTCTTTCCCTAGCT
SOX2	Forward	CCCAGCAGACTTCACATGT
	Reverse	CCTCCCATTTCCCTCGTTTT
TERT	Forward	CTGGAGCAAGTTGCAAAGC
	Reverse	GTCCATGTTCACAATCGGC
PCR primers for plasmid residual and random integration test		
Gene	Sequence (5'→3')	
MYC	Forward	TCAAGAGGCGAACACACAAC
	Reverse	AGGAACTGCTTCCTTCACGA
EBNA-1	Forward	ATCGTCAAAGCTGCACACAG
	Reverse	CCCAGGAGTCCCAGTAGTCA
KLF4	Forward	CCCACACAGGTGAGAAACCT
	Reverse	CCCCCTGAACCTGAAACATA
LIN28	Forward	AAGCGCAGATCAAAAGGAGA
	Reverse	CCCCCTGAACCTGAAACATA
OCT4	Forward	AGTGAGAGGCAACCTGGAGA
	Reverse	AGGAACTGCTTCCTTCACGA
Endo-*OCT4*	Forward	AGTTTGTGCCAGGGTTTTTG
	Reverse	ACTTCACCTTCCCTCCAACC
OriP	Forward	TTCCACGAGGGTAGTGAACC
	Reverse	TCGGGGGTGTTAGAGACAAC
SOX2	Forward	ACCAGCTCGCAGACCTACAT
	Reverse	CCCCCTGAACCTGAAACATA
SV40LT	Forward	TGGGGAGAAGAACATGGAAG
	Reverse	AGGAACTGCTTCCTTCACGA
RT-qPCR primers for mouse proinflammatory genes		
Gene	Sequence (5'→3')	
Ccl8	Forward	TTCTTTGCCTGCTGCTCATA
	Reverse	AGCAGGTGACTGGAGCCTTA
Ccr2	Forward	ACCAGAAGAGGGCATTGGAT
	Reverse	GCCGTGGATGAACTGAGGTA
Ccl2	Forward	CATCCACGTGTTGGCTCA
	Reverse	GATCATCTTGCTGGTGAATGAGT
S100a8	Forward	TCCTTTGTCAGCTCCGTCTT
	Reverse	AGAGGGCATGGTGATTTCCT
Icam1	Forward	GTGATGCTCAGGTATCCATCCA
	Reverse	CACAGTTCTCAAAGCACAGCG
Vcam1	Forward	CCGGCATATACGAGTGTGAA
	Reverse	GGAGTTCGGGCGAAAAATAG
Sele	Forward	CAGCTTCGTGTACCAATGCA
	Reverse	GGCTTCCATAGTCAGGGTGT
Gapdh	Forward	ATGGTGAAGGTCGGTGTGAA
	Reverse	GAGGTCAATGAAGGGGTCGT
PCR primers for isogenic *LDLR* knockout clone screening		

Gene	Sequence (5’→3’)		
LDLR	Forward		AGCTTCCAGTGCAACAGCTC
	Reverse		AAATCACTGCATGTCCCACA
	Sequencing primer		AGCTTCCAGTGCAACAGCTC
PCR primers for bisulfite sequencing			
Gene	Sequence (5’→3’)		
NANOG promoter	Inner	Forward	TTAATTTATTGGGATTATAGGGGTG
		Reverse	AACAACAAAACCTAAAAACAAACC
	Outer	Forward	TGGTTAGGTTGGTTTTAAATTTTTG
		Reverse	AACCCACCCTTATAAATTCTCAATTA

Supplemental Table S2

List of Antibodies Used in this Study

Primary antibodies			
Name	**Dilution**	**Vendor (cat#)**	
Immunofluorescence staining (IF) and immunohistochemistry (IHC)			
Rabbit anti-A1AT	1:100	Invitrogen (18-0002)	
Rabbit anti-ASGPR	1:100	Santa Cruz (Sc-28977)	
Mouse anti-ASGPR	1:25	Santa Cruz (Sc-166633)	
Goat anti-HNF4A	1:35	Santa Cruz (Sc-6557)	
Goat anti-hALB	1:200	Bethyl Laboratories (A80-129)	
Mouse anti-hNA	1:200	Millipore (MAB1281)	
Rabbit anti-LDLR	1:200	Novus Biologicals (NB110-57162)	
Rabbit anti-NANOG	1:200	Stemgent (09-0020)	
Mouse anti-SSEA-4	1:200	Stemgent (09-0006)	
Western blotting (WB)			
Rabbit anti-LDLR	1:2000	Novus Biologicals (NB110-57162)	
Rabbit anti-ACTIN	1:1000	Sigma Aldrich (A2066)	
Mouse anti-PCSK9	1:1000	Cayman Chemical (10218)	
***In-vitro* drug testing**			
Mouse anti-PCSK9	0.02 μM, 0.20 μM, and 2.00 μM	Cayman Chemical (10218)	
***In-vivo* drug testing**			
Humanized monoclonal antibody anti-human PCSK9	10 mg/kg mouse	Sanofi and Regeneron Pharmaceuticals (SAR236553/REGN727)	
Secondary antibodies			
Name	**Dilution**	**Vendor (cat#)**	**Applications**
Donkey anti-goat Alexa Fluor 594	1:1000	Invitrogen (A11058)	IF
Donkey anti-rabbit Alexa Fluor 488	1:1000	Invitrogen (A21206)	IF/IHC
Goat anti-mouse Alexa Fluor 488	1:1000	Invitrogen (A10667)	IF
Goat anti-rabbit Alexa Fluor 594	1:1000	Invitrogen (A11072)	IF
Rabbit anti-goat Alexa Fluor 488	1:1000	Invitrogen (A21222)	IF/IHC
Rabbit anti-mouse Alexa Fluor 594	1:1000	Invitrogen (A11062)	IF/IHC
Rabbit anti-mouse Alexa Fluor 488	1:1000	Invitrogen (A11059)	IF/IHC
EnVision goat anti-rabbit HRP	No dilution	DAKO (K4003)	IHC
EnVision goat anti-mouse HRP	No dilution	DAKO (K4001)	IHC
Rabbit anti-goat HRP	1:1000	DAKO (P0449)	IHC
Goat anti-mouse HRP	1:5000	Invitrogen (A16072)	WB
Goat anti-rabbit HRP	1:5000	Invitrogen (A16104)	WB

SUPPLEMENTAL EXPERIMENTAL PROCEDURES

Knockout iPSC Generation

iPSCs were dissociated into single cells with Accutase (Sigma-Aldrich) and transfected with 8 μg *LDLR*-ZFN encoding mRNAs through nucleofection (Amaxa™ Nucleofector™ I with Human Stem Cell Nucleofector® Kit 2 VPH-5022 under program A23). Cells were maintained for 48-72 hours under 30°C and 5% CO2 transient cold shock conditions (Doyon et al., 2010) in the presence of ROCK inhibitor Y27632 (Sigma-Aldrich), and then transferred to 37°C and 5% CO_2 conditions for recovery. Cell cultures were dissociated into single cells and seeded onto 96-well plates by limited dilution to obtain single cell-derived subclones. Genotype of the individual subclones was confirmed by PCR and sequencing of the *LDLR*-ZFN target site. Clones with biallelic and monoallelic frameshift mutations were selected for further analysis.

RNA Isolation, RT-qPCR Analysis, DNA Methylation Analysis, and Teratoma Formation

Total RNA was extracted from cell lysates or tissue in TRI Reagent® Solution (Invitrogen). cDNA was obtained from 1 mg of total RNA using PrimeScript™ Double Strand cDNA Synthesis Kit (Takara) and RT-qPCR was performed using a Thermal Cycler Dice™ real-time system (ABI7300, ABI) and SYBR Green Premix EX Taq™ (Takara). *ACTB or Gapdh* was used for normalization, and items were measured in triplicate. *NANOG* promoter DNA methylation analysis was performed using bisulfite-assisted genomic sequencing method (Hajkova et al., 2002). All primers used in this study are listed in *Supplemental Table S1*. For teratoma formation, cells were dissociated with Accutase and suspended in 30% Matrigel in Ca^{2+}/Mg^{2+} free PBS (CMF-PBS, Hyclone), then 3 million cells were injected subcutaneously into the flanks of SCID mice. Tumors were dissected and sectioned 7-9 weeks later, and then stained with hematoxylin/eosin (Sigma-Aldrich).

PAS Staining, Immunofluorescence, and Western Blotting

After 17 days of iHep differentiation, PAS staining on iHeps was performed using Periodic Acid-Schiff Kit (Sigma-Aldrich) according to the manufacturer's specifications. Immunofluorescence and Western blotting were performed following standard procedures. For immunofluorescence, cells were fixed in 4% paraformaldehyde (Affymetrix) for 10 minutes at room temperature. Nuclei were stained with DAPI (Sigma-Aldrich). Primary and second antibodies for both procedures are listed in *Supplemental Table S2*.

LDL Uptake Assays

Briefly, iHeps at day 17 of differentiation were washed 3 times with cold CMF-PBS rapidly. Then, ice-cold HCM medium supplemented with 5 μg/ml FL LDL or DiI LDL was added, and the plates were incubated on ice for 5 minutes before transferring to a 37°C and 5% CO_2 incubator for 3.5 hours. Then, cells were washed with ice-cold CMF-PBS for 3 times. For FL LDL monitoring under the fluorescence microscope, iHeps were fixed with 4% paraformaldehyde for 10 minutes at room temperature and then co-stained with anti-HNF4A according to the immunofluorescence protocol described above. For quantification of DiI $LDL^+/ASGPR^+$ iHeps, after DiI LDL capture, iHeps were fixed and permeabilized with Cytofix/Cytoperm™ Fixation/Permeabilization Kit (BD), and stained with ASGPR antibodies. Ratios of DiI $LDL^+/ASGPR^+$ iHeps were quantified by flow cytometry.

Oil Red O Staining, Urea Secretion, and CYP3A4 Activity

For Oil Red O staining, iHeps at day 17 of differentiation were washed 3 times with CMF-PBS, and then fixed in 4% paraformaldehyde for 10 minutes at room temperature. Cells were subjected to Oil Red O (Sigma-Aldrich) staining for 15 minutes after 3 washes with deionized distilled water, and then stained with hematoxylin for 5 minutes after another 3 rounds of washing. Urea secretion was detected directly on culture medium of iHeps at day 17 of differentiation with Urea Assay Kit (Sigma-Aldrich) according to the manufacturer's specifications. Culture medium of iHeps was used as control. CYP3A4 activity was measured using P450-Glo Assays kit (Promega) according to the manufacturer's specifications. Briefly, iHeps at day 17 of differentiation were pretreated with 25 μM rifampicin or vehicle (DMSO) for 72 hours, and then were incubated with fresh medium containing the luminogenic CYP3A4 substrate Luciferin-IPA at 37°C for 1 hour. Then, 25 μl of culture medium were transferred to a 96-well white luminometer-plate, and 25 μl of Luciferin Detection Reagent was added to initiate the luminescent reaction. Luminescence was measured using a CLARIOstar microplate reader (BMG LABTECH) 20 minutes later. Relative light units (RLU)/10^6 cells/ml indicate CYP3A4 activity.

Histology and Immunohistochemistry

Mice were sacrificed by carbon dioxide asphyxiation, and livers were perfused and fixed with 10% formalin solution (Sigma-Aldrich), embedded in paraffin (Leica Biosystems), sectioned and stained with primary antibodies. Secondary antibodies conjugated with fluorescent labels or HRP, which react with DAB detection kit (Invitrogen), were used for immunostaining of chimeric liver sections. Primary and secondary antibodies for immunohistochemistry are listed in *Supplemental Table S2*. Quantification of the percentage of hNA+ cells was based on 10 regions/mouse (randomly selected) and performed by manual counting in Adobe Photoshop (version 2015.0.0). Slides stained with anti-hALB and reacted with DAB were scanned by Aperio ScanScope System (Leica Biosystems). For hALB+ area quantification, images

of whole slides were divided into pieces by snapshot and then quantified by Zeiss AxioVision LE, the edge of the lobes was excluded when doing quantification. Counts were based on no less than 4 sections of liver lobes and lobules per mice, and 3-5 mice per group.

Functional Studies in Myograph

Briefly, after mice were anaesthetized with ketamine/xylazine, the thoracic aortae were dissected in oxygenated ice-cold Krebs-Henseleit solution (mM: 119 NaCl, 4.7 KCl, 2.5 $CaCl_2$, 1 $MgCl_2$, 25 $NaHCO_3$, 1.2 KH_2PO_4, and 11 D-glucose). Changes in isometric tension of arteries were measured and recorded in a multi-myograph system (Danish Myo Technology) as described previously (Wong et al., 2010). The aortic ring (~1.5 mm in length) was stretched to basal tension ~3 mN and equilibrated for 1 hour before the experiment. Then, aortic rings were first contracted by 60 M KCl and rinsed in Krebs solution for 3 times. EDV to accumulative concentrations of Ach (10 nM to 10 μM) was examined in Phe (3 μM)-contracted aortic rings. Endothelium-independent relaxations to sodium nitroprusside (SNP) (1 nM to 10 μM) were recorded in endothelium-denuded rings.

SUPPLEMENTAL REFERENCES

Doyon, Y., Choi, V.M., Xia, D.F., Vo, T.D., Gregory, P.D., and Holmes, M.C. (2010). Transient cold shock enhances zinc-finger nuclease-mediated gene disruption. Nat. Methods *7*, 459-460.

Hajkova, P., el-Maarri, O., Engemann, S., Oswald, J., Olek, A., and Walter, J. (2002). DNA-methylation analysis by the bisulfite-assisted genomic sequencing method. Methods Mol. Biol. *200*, 143-154.

Wong, W.T., Tian, X.Y., Xu, A., Ng, C.F., Lee, H.K., Chen, Z.Y., Au, C.L., Yao, X., and Huang, Y. (2010). Angiotensin II type 1 receptor-dependent oxidative stress mediates endothelial dysfunction in type 2 diabetic mice. Antioxid. Redox Signal. *13*, 757-768.